

NASA/TP-2008-215555



Cross Sections From Scalar Field Theory

Frank Dick
Worcester Polytechnic Institute, Worcester, Massachusetts

John W. Norbury
Langley Research Center, Hampton, Virginia

Ryan B. Norman
University of Tennessee, Knoxville, Tennessee

Rachel Nasto
Worcester Polytechnic Institute, Worcester, Massachusetts

The NASA STI Program Office . . . in Profile

Since its founding, NASA has been dedicated to the advancement of aeronautics and space science. The NASA Scientific and Technical Information (STI) Program Office plays a key part in helping NASA maintain this important role.

The NASA STI Program Office is operated by Langley Research Center, the lead center for NASA's scientific and technical information. The NASA STI Program Office provides access to the NASA STI Database, the largest collection of aeronautical and space science STI in the world. The Program Office is also NASA's institutional mechanism for disseminating the results of its research and development activities. These results are published by NASA in the NASA STI Report Series, which includes the following report types:

- **TECHNICAL PUBLICATION.** Reports of completed research or a major significant phase of research that present the results of NASA programs and include extensive data or theoretical analysis. Includes compilations of significant scientific and technical data and information deemed to be of continuing reference value. NASA counterpart of peer-reviewed formal professional papers, but having less stringent limitations on manuscript length and extent of graphic presentations.
- **TECHNICAL MEMORANDUM.** Scientific and technical findings that are preliminary or of specialized interest, e.g., quick release reports, working papers, and bibliographies that contain minimal annotation. Does not contain extensive analysis.
- **CONTRACTOR REPORT.** Scientific and technical findings by NASA-sponsored contractors and grantees.

- **CONFERENCE PUBLICATION.** Collected papers from scientific and technical conferences, symposia, seminars, or other meetings sponsored or co-sponsored by NASA.
- **SPECIAL PUBLICATION.** Scientific, technical, or historical information from NASA programs, projects, and missions, often concerned with subjects having substantial public interest.
- **TECHNICAL TRANSLATION.** English-language translations of foreign scientific and technical material pertinent to NASA's mission.

Specialized services that complement the STI Program Office's diverse offerings include creating custom thesauri, building customized databases, organizing and publishing research results ... even providing videos.

For more information about the NASA STI Program Office, see the following:

- Access the NASA STI Program Home Page at <http://www.sti.nasa.gov>
- E-mail your question via the Internet to help@sti.nasa.gov
- Fax your question to the NASA STI Help Desk at (301) 621-0134
- Phone the NASA STI Help Desk at (301) 621-0390
- Write to:
NASA STI Help Desk
NASA Center for AeroSpace Information
7115 Standard Drive
Hanover, MD 21076-1320

NASA/TP-2008-215555



Cross Sections From Scalar Field Theory

Frank Dick
Worcester Polytechnic Institute, Worcester, Massachusetts

John W. Norbury
Langley Research Center, Hampton, Virginia

Ryan B. Norman
University of Tennessee, Knoxville, Tennessee

Rachel Nasto
Worcester Polytechnic Institute, Worcester, Massachusetts

National Aeronautics and
Space Administration

Langley Research Center
Hampton, Virginia 23681-2199

December 2008

Available from:

NASA Center for AeroSpace Information (CASI)
7115 Standard Drive
Hanover, MD 21076-1320
(301) 621-0390

National Technical Information Service (NTIS)
5285 Port Royal Road
Springfield, VA 22161-2171
(703) 605-6000

Nomenclature

Note: Units are used in which $c = \hbar = 1$.

c	speed of light
\hbar	Planck constant divided by 2π
l, lab	as a subscript, refers to lab frame
c, cm	as a subscript, refers to center of mass frame
λ_{ij}	flux factor for masses i and j
E_i	energy of particle i
\mathbf{p}_i	3-momentum of particle i
p_i	4-momentum of particle i
q_j	4-momentum of virtual particle j
\mathcal{M}	invariant amplitude
g	coupling constant
g_{13x}	coupling constant between particles 1, 3 and exchange particle x
$g_{\pi NN}$	pion-nucleon coupling constant
$g_{\pi N\Delta}$	pion-nucleon-delta coupling constant
$g_{\gamma NN}$	electromagnetic coupling constant
m_j	mass of particle j
m_Δ	mass of the Δ particle
m_π	mass of the pion
m_x	mass of the exchange particle (e.g. $x = \pi$, the pion)
m_p	mass of the proton
m_N	mass of a nucleon
Γ	total decay width or rate
$\Gamma(4 \rightarrow 56)$	partial decay width for exclusive decay $4 \rightarrow 56$
$d\Gamma$	differential decay width
\mathcal{S}	statistical factor
σ	total cross section
σ_d	total cross section due to direct term
σ_e	total cross section due to exchange term
σ_i	total cross section due to interference term
$d\sigma$	infinitesimal element of differential cross section
$d\sigma/dt$	invariant differential cross section
$d\sigma/d\Omega$	angular distribution
$d\sigma/dE_i$	spectral distribution in terms of energy of particle i
$d\sigma/dT_j$	spectral distribution in terms of kinetic energy of particle j
N	a nucleon
θ_{3l}	lab angle of particle 3 with respect to particle 1
θ_{4c}	cm angle of particle 4 with respect to particle 1
$\theta_{3\text{peak}}$	maximum angle of particle 3 with respect to particle 1
s, t, u	mandelstam variables
t_0	value of variable t at $\theta = 0$

t_π	value of variable t at $\theta = \pi$
u_0	value of variable u at $\theta = 0$
u_π	value of variable u at $\theta = \pi$
s_t	$= s_{\text{threshold}}$, value of variable s at the reaction threshold
π^0	the neutral pion
Δ^+	the Δ baryon of charge +1
γ	the photon
GeV	mass energy unit, one billion electron volts
mb	millibarns
pb	picobarns
sr	steradian, unit of solid angle
$d\Phi_2$	phase space factor for 2 particle final state
$d\Phi_n$	phase space factor for n particle final state
$dLips$	Lorentz invariant phase space factor
τ	mean lifetime
OPE	one pion exchange

$$\Sigma m^2 \equiv \sum_{i=1}^4 m_i^2 \equiv m_1^2 + m_2^2 + m_3^2 + m_4^2$$

Contents

1	Introduction	1
2	Scattering for 2 - body final states	1
2.1	Scattering amplitude from Feynman rules	2
2.2	Decay width from Feynman rules	3
2.3	Scattering via massive exchange particle	4
2.3.1	Amplitude	4
2.3.2	Invariant t distribution	6
2.3.3	Spectral distribution in the lab frame	8
2.3.4	Angular distribution in the cm frame	8
2.3.5	Angular distribution in the lab frame	9
2.3.6	Singularities	10
2.4	Scattering via zero-mass exchange particle	13
2.5	Total cross section	14
2.5.1	Asymptotic region	20
3	Calculations for 2 - body final states	20
3.1	Coupling constants	20
3.2	Calculations for scattering involving a massive exchange particle	20
3.2.1	Minimum and maximum values of t	21
3.2.2	Singularities	21
3.3	Invariant distribution $d\sigma/dt$	22
3.4	Angular distribution $d\sigma/d\Omega_c$ and σ in cm frame	24
3.5	Spectral distribution $d\sigma/dE_{3l}$ in the lab frame	26
3.6	Angular distribution $d\sigma/d\Omega_{3l}$ in lab frame	27
3.6.1	Relation between cm and lab angles	28
3.7	Calculations for zero-mass exchange particle (Rutherford scattering)	30
3.8	Comparison of cross sections	31
4	Scattering for 3 - body final states	33
4.1	Amplitude for Δ resonance formation and decay	35
4.2	Cross section for resonance formation and decay	38
4.2.1	Integration bounds on p_4^2	40
4.2.2	Alternate derivation of the cross section	41
4.2.3	Narrow width approximation	42
4.3	$dLips$ formalism	43
4.4	Proof of phase space formula	43
5	Conclusions	45

List of Figures

1	Lowest order contribution to the decay $3 \rightarrow 1 + 2$	3
2	Lowest order contribution to the reaction $1 + 2 \rightarrow 3 + 4$	4
3	Exchange term of reaction $1 + 2 \rightarrow 3 + 4$	5
4	Differential cross section $d\sigma/dt$	23
5	Differential cross section $d\sigma/dt$ direct term.	23
6	Differential cross section $d\sigma/dt$ exchange term.	24
7	$pp \rightarrow p\Delta^+$ total cross section.	24
8	Differential cross section $d\sigma/d\Omega_{4c}$	25
9	Total cross section σ	26
10	Differential cross section $d\sigma/dE_{4l}$	27
11	Energy $E_{3l}(\theta_{3l})$. Upper and lower parts of the curve correspond to E_{3l} roots 1 and 2, respectively.	28
12	Differential cross section $d\sigma/d\Omega_{3l}$	29
13	Detector partial cross section.	29
14	Angles θ_{3lab} and θ_{4lab} versus θ_{cm}	30
15	Mandelstam variable t as a function of θ_{3l}	30
16	Mandelstam variable u as a function of θ_{3l}	31
17	Invariant differential cross section (non-Rutherford).	32
18	$d\sigma/d\Omega_{cm}$ Differential cross section (non-Rutherford).	32
19	Invariant differential cross section (Rutherford).	33
20	$d\sigma/d\Omega_{cm}$ Differential cross section (Rutherford)	33
21	Total cross section (non-Rutherford).	34
22	Comparison of elastic and inelastic total cross sections. The steadily falling cross section is elastic, and the cross section which rises and then falls is inelastic.	34
23	Invariant distribution for $pp \rightarrow pp$ by pion exchange.	35
24	Invariant distribution for $pp \rightarrow pp$ by photon exchange.	35
25	The Feynman diagram for the reaction $NN \rightarrow N\Delta \rightarrow NN\pi$. Note the labeling of the particle numbers. The initial state nucleons are labeled as particles 1 and 2. The final state nucleons are labeled as particles 3 and 5. The intermediate Δ state is labeled as particle 4, and the final produced π is labeled as particle 6.	36
26	The Feynman diagram for the reaction $NN \rightarrow N\Delta$	37
27	The Feynman diagram for the decay $\Delta \rightarrow N\pi$	38

List of Tables

1	Values of t and u for $\theta_{3lab} = 0.4$	5
---	---	---

Abstract

A one pion exchange scalar model is used to calculate differential and total cross sections for pion production through nucleon-nucleon collisions. The collisions involve intermediate delta particle production and decay to nucleons and a pion. The model provides the basic theoretical framework for scalar field theory and can be applied to particle production processes where the effects of spin can be neglected.

1 Introduction

An effort is underway to include meson production in the space radiation transport code known as HZETRN. Previous work used high energy meson production models based on scaling [1, 2, 3, 4, 5]. These models yield nucleon, pion, and other particle production cross sections. Basing the transport codes instead on fundamental models of hadronic interactions holds out the prospect of providing unified and more versatile descriptions of the interactions of interest. The quark - gluon model is the most fundamental, but its complexities are such that calculations are more of a qualitative kind [6]. The present work is based on the meson exchange model of hadronic (strong) interactions [6]. The model may be considered an effective quantum field theory in which the exchange particle is the pion. In the model's simplest form, all particles, nucleons and exchange particles alike, are treated as scalar, spin zero particles. This version of the model makes no distinction between proton and neutron other than by mass, but since the masses are nearly equal, the mass of the proton is used throughout as the nucleon mass. As a further simplification, only the pion is used as the exchange particle. This scalar one pion exchange (OPE) model is used to determine the amplitudes, to first and second order in coupling constants, of Δ decays and nucleon - nucleon (NN) interactions producing 2 - body and 3 - body final states. The amplitudes are inserted into standard formulas derived from Fermi's golden rule to give differential decay widths for $\Delta \rightarrow N\pi$ and differential cross sections for the elastic $NN \rightarrow NN$ and inelastic $NN \rightarrow N\Delta$ interactions. Manipulation of the phase space factor in the differential cross section leads to an expression for the invariant distribution, a differential cross section that is a function of Mandelstam variable t . Changes of variable lead to angular distributions in the center of momentum (cm) frame and angular and spectral distributions in the lab frame. Of the various distributions, the invariant distribution reveals itself to have a particularly simple form. Allowed ranges of variables are found, and integration over the variables yields total cross sections.

2 Scattering for 2 - body final states

In 2 - body decay, the lowest order term in the scattering matrix has one vertex, and thus is first order in the coupling constant $g_{\pi NN}$. In 2 - body scattering, the lowest order term in the scattering matrix has two vertices, and thus is second order in the coupling constant. 2 - body reactions will be represented as $1 + 2 \rightarrow 3 + 4$, where the numbers represent particles. Both decay and scattering processes have a 2 - body final state. In this section, the basic formalism for calculating 2 - body final state cross sections is presented.

2.1 Scattering amplitude from Feynman rules

In this subsection, it will be shown how to generate a scattering amplitude from a set of Feynman rules. This amplitude is the basic input to physical observables, such as cross sections and decay rates. The Feynman rules used below apply to a set of particles that are scalars. Griffiths [7] labels the particles as A, B, C each with different masses. The exchange particle is particle C . We consider the Feynman rules for the scalar ABC theory of Griffiths [7]. The rules of Peskin and Schroeder [8] and Griffiths [7] are the same except that Griffiths has rules leading to the invariant amplitude $-i\mathcal{M}$, whereas Peskin and Schroeder have the rules giving $+i\mathcal{M}$. This discrepancy is due to different definitions relating the S-matrix to the invariant amplitude. We follow the convention of Peskin and Schroeder in the present work. Another difference is that Peskin and Schroeder always include a factor $i\epsilon$ in the denominator of propagators. We include this factor in the form $im\Gamma$ in the case of Δ decay to account for the decay width. The Feynman rules are now discussed. The quantity

$$i\mathcal{M}(2\pi)^4\delta^4(p_1 + p_2 - p_3 - p_4 \cdots - p_n), \quad (1)$$

is given by the following rules [7, 8] for scalar ABC theory [7].

1. Notation. Label the incoming 4-momenta as p_1 and p_2 , and the outgoing momenta as $p_3, p_4 \cdots p_n$. Label the internal 4-momenta as $q_1, q_2 \dots$. Put arrows on each line to conserve current, which identify incoming and outgoing particles.
2. Coupling constant. For each vertex, write down a factor

$$-ig$$

where g is the coupling constant. (In our simple scalar theory, this has dimensions of GeV, but in realistic theories g is always dimensionless. In the theory of Quantum Electrodynamics, g is the fine structure constant $\alpha \cong 1/137$.)

3. Propagator. For each internal line, write a factor

$$\frac{i}{q_j^2 - m_j^2 + i\epsilon}$$

where q_j is the 4-momentum of the internal particle and m_j is its mass. Note that $q_j^2 \neq m_j^2$, because the internal particle is virtual and does not obey the Einstein relation, $p^2 = m^2$. We say that such a particle is off mass shell. Also, as mentioned above, the factor $i\epsilon$ is omitted except in the case where decay width is significant.

4. Conservation of 4-momentum. At each vertex, write a delta function of the form

$$(2\pi)^4\delta^4(k_1 + k_2 + k_3)$$

where the k 's are the 4-momenta flowing into the vertex. If the particle flows out, then k should have a negative sign in front.

5. Integrate over internal momenta. For each internal line, write down a factor

$$\frac{1}{(2\pi)^4} d^4 q_j$$

and integrate over all internal momenta.

2.2 Decay width from Feynman rules

Most baryons decay into a final set of particles. Therefore, it is important to be able to describe this decay. This subsection shows how to calculate the decay width from Feynman rules. The Feynman rules may be used to calculate the decay width of particle 3 decaying, as in the reaction

$$3 \rightarrow 1 + 2 . \quad (2)$$

The Feynman diagram for this reaction is shown in figure 1. This diagram is particularly easy to evaluate since there are no internal lines. Applying the Feynman rules to the lowest order diagram (see Griffiths [7]), gives

$$i\mathcal{M}(2\pi)^4 \delta^4(p_1 - p_2 - p_3) = (-ig)(2\pi)^4 \delta^4(p_1 - p_2 - p_3) , \quad (3)$$

and canceling terms gives

$$\mathcal{M} = -g . \quad (4)$$

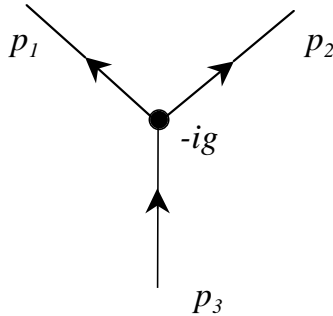


Figure 1: Lowest order contribution to the decay $3 \rightarrow 1 + 2$.

Step 5 in section 2.1 is not needed because there are no internal particles for the first order decay. Substituting equation (4) into equation 6.30 of Reference [7] gives

$$\Gamma = \frac{1}{\tau} = \frac{g_{\pi N \Delta}^2 \mathcal{S}}{16\pi m_3^3} \sqrt{m_1^4 + m_2^4 + m_3^4 - 2m_1^2 m_2^2 - 2m_1^2 m_3^2 - 2m_2^2 m_3^2} , \quad (5)$$

where $g = g_{\pi N \Delta}$.

2.3 Scattering via massive exchange particle

In this section, we consider scattering by means of an exchange particle with mass $m > 0$. Since the exchange particle is a virtual particle, its mass is allowed to be off-shell. In the case of the pion, this means that the square of the 4-momentum transferred by the virtual pion $t = (p_1 - p_3)^2$ is in general not equal to the squared mass of a real pion, $t \neq m_\pi^2$. In treating the reaction $NN \rightarrow N\Delta$, the ABC theory is simply expanded to include two types of vertices, along with their respective coupling constants: $NN\pi$ and $N\Delta\pi$.

2.3.1 Amplitude

Consider the reaction

$$1 + 2 \rightarrow 3 + 4 ,$$

with the diagram shown in figure 2. The particles have masses m_1, m_2, m_3 and m_4 , respectively, and the mass of the intermediate exchange particle is m_x . Applying the Feynman rules to the lowest order diagram (see Reference [7]), gives the direct amplitude as

$$\begin{aligned} & i\mathcal{M}_d(2\pi)^4\delta^4(p_1 + p_2 - p_3 - p_4) \\ = & (-i)^2 g_{13x}g_{24x} \int \frac{d^4q}{(2\pi)^4} \frac{i}{q^2 - m_x^2} (2\pi)^4\delta^4(p_1 - p_3 - q)(2\pi)^4\delta^4(q + p_2 - p_4) \\ = & (-i)^2 g_{13x}g_{24x} \frac{i}{(p_1 - p_3)^2 - m_x^2} (2\pi)^4\delta^4(p_1 - p_3 + p_2 - p_4) , \end{aligned} \quad (6)$$

and canceling terms gives

$$\mathcal{M}_d = -\frac{g_{13x}g_{24x}}{t - m_x^2} , \quad (7)$$

where $t \equiv (p_1 - p_3)^2$.

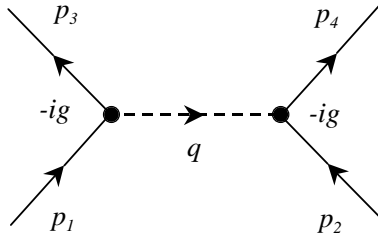


Figure 2: Lowest order contribution to the reaction $1 + 2 \rightarrow 3 + 4$.

The exchange term is shown in figure 3 and is given by

$$\mathcal{M}_e = \frac{g_{14x}g_{23x}}{(p_1 - p_4)^2 - m_x^2} = +\frac{g_{14x}g_{23x}}{u - m_x^2} , \quad (8)$$

where $u \equiv (p_1 - p_4)^2$. The plus sign of the exchange term in equation (8) is consistent with the scalar theory in which all particles are spin 0 bosons with wave functions that commute. Had spin been considered, then for the case of nucleon scattering, in which the nucleons are fermions with spin 1/2, the exchange term in equation (8) would have taken on a minus sign reflecting the fact that the wave functions of the two fermions anti-commute [8] (p. 119).

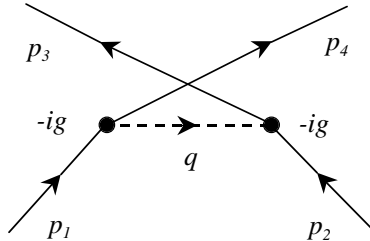


Figure 3: Exchange term of reaction $1 + 2 \rightarrow 3 + 4$.

For the reaction $NN \rightarrow NN$, the direct and exchange terms are physically indistinguishable in so much as the energies and exit angles of a final state particle are the same for both terms. According to the rules of quantum mechanics, the probability (i.e. cross section) to produce the final state particles is determined by first adding the amplitudes of the two terms, and then squaring the complete amplitude, (rather than the reverse, as would be the case for distinguishable final states [9] (p. 10).

Table 1: Values of t and u for $\theta_{3lab} = 0.4$

$E_{3lab}(\text{GeV})$	$t(\text{GeV}^2)$	$u(\text{GeV}^2)$
2.98	- 2.07	- 3.19
1.30	- 5.23	- 0.035

For each energy, there is a unique value of t that determines that energy. This value of t represents the direct term. There is also a unique value of u that determines that energy. See Table 1. This value of u represents the exchange term. The invariant amplitude \mathcal{M} consists of the sum of direct (t -channel) and exchange (u -channel) terms and is finally

$$\mathcal{M} \equiv \mathcal{M}_d + \mathcal{M}_e = -\frac{g_{13x}g_{24x}}{t - m_x^2} + \frac{g_{14x}g_{23x}}{u - m_x^2}. \quad (9)$$

The Mandelstam variables s, t, u satisfy

$$s + t + u = m_1^2 + m_2^2 + m_3^2 + m_4^2 = \sum_{i=1}^4 m_i^2 \equiv \Sigma m^2, \quad (10)$$

where $s \equiv (p_1 + p_2)^2$.

2.3.2 Invariant t distribution

Final formulas for the Lorentz invariant angular cross sections will now be presented. Reference [10] gives

$$\frac{d\sigma}{dt} = \frac{\mathcal{S}}{16\pi\lambda_{12}} |\mathcal{M}|^2 = \frac{\mathcal{S}}{16\pi\lambda_{12}} \left[\frac{g_{13x}g_{24x}}{t - m_x^2} + \frac{g_{14x}g_{23x}}{u - m_x^2} \right]^2, \quad (11)$$

with

$$\lambda_{ij} \equiv (s - m_i^2 - m_j^2)^2 - 4m_i^2 m_j^2. \quad (12)$$

The direct, exchange, and interference terms are

$$\frac{d\sigma_d}{dt} = \frac{\mathcal{S}}{16\pi\lambda_{12}} |\mathcal{M}_d|^2 = \frac{\mathcal{S}}{16\pi\lambda_{12}} \frac{g_{13x}^2 g_{24x}^2}{(t - m_x^2)^2}, \quad (13)$$

$$\frac{d\sigma_e}{dt} = \frac{\mathcal{S}}{16\pi\lambda_{12}} |\mathcal{M}_e|^2 = \frac{\mathcal{S}}{16\pi\lambda_{12}} \frac{g_{14x}^2 g_{23x}^2}{(u - m_x^2)^2}, \quad (14)$$

$$\frac{d\sigma_i}{dt} = \frac{\mathcal{S}}{16\pi\lambda_{12}} |\mathcal{M}_i|^2 = \frac{\mathcal{S}}{16\pi\lambda_{12}} 2\mathcal{M}_d \mathcal{M}_e = \frac{\mathcal{S}}{16\pi\lambda_{12}} \frac{2g_{13x}g_{24x}g_{14x}g_{23x}}{(t - m_x^2)(u - m_x^2)}. \quad (15)$$

For future purposes, we write these more simply as

$$\frac{d\sigma_d}{dt} = \frac{K}{(t - m_x^2)^2}, \quad (16)$$

$$\frac{d\sigma_e}{dt} = \frac{K}{(u - m_x^2)^2}, \quad (17)$$

$$\frac{d\sigma_i}{dt} = \frac{2K}{(t - m_x^2)(u - m_x^2)}, \quad (18)$$

with the definition

$$K \equiv K(s) \equiv \frac{\mathcal{S}}{16\pi\lambda_{12}} g_{13x}^2 g_{24x}^2 = \frac{\mathcal{S} g_{13x}^2 g_{24x}^2}{16\pi[(s - m_1^2 - m_2^2)^2 - 4m_1^2 m_2^2]}, \quad (19)$$

which assumes

$$g_{23x} \equiv g_{13x}, \quad (20)$$

$$g_{24x} \equiv g_{14x}. \quad (21)$$

This equivalence of coupling constants between the direct and exchange terms assumes particles 1 and 2 are the same. This is the case for the following discussions in which the particles are both nucleons. $K(s)$ has a singularity when $(s - m_1^2 - m_2^2)^2 - 4m_1^2m_2^2 = 0$, and it will turn out that this gets canceled by other terms. See the note following equation (111).

Elastic scattering (e.g. $NN \rightarrow NN$)

Consider the example of the reaction $NN \rightarrow NN$ where the exchange particle is a pion,

$$g_{13x} = g_{24x} = g_{NN\pi} \equiv g_{\pi NN} , \quad (22)$$

$$m_1 = m_2 = m_3 = m_4 \equiv m_N , \quad (23)$$

$$m_x = m_\pi \equiv m , \quad (24)$$

$$\mathcal{S} = 1/2 , \quad (25)$$

which gives

$$\lambda_{12} = s(s - 4m_N^2) , \quad (26)$$

and

$$K = \frac{\mathcal{S}}{16\pi\lambda_{12}} g_{13x}^2 g_{24x}^2 = \frac{g_{\pi NN}^4}{32\pi s(s - 4m_N^2)} . \quad (27)$$

Inelastic scattering (e.g. $NN \rightarrow N\Delta$)

Consider the example of the reaction $NN \rightarrow N\Delta$ where the exchange particle is a pion,

$$g_{13x} = g_{NN\pi} \equiv g_{\pi NN} , \quad (28)$$

$$g_{24x} = g_{N\Delta\pi} \equiv g_{\pi N\Delta} , \quad (29)$$

$$m_1 = m_2 = m_3 \equiv m_N , \quad (30)$$

$$m_4 \equiv m_\Delta , \quad (31)$$

$$m_x = m_\pi \equiv m , \quad (32)$$

$$\mathcal{S} = 1 , \quad (33)$$

which gives

$$\lambda_{12} = s(s - 4m_N^2) , \quad (\text{same as elastic case}), \quad (34)$$

and

$$K = \frac{\mathcal{S}}{16\pi\lambda_{12}} g_{13x}^2 g_{24x}^2 = \frac{g_{\pi NN}^2 g_{\pi N\Delta}^2}{16\pi s(s - 4m_N^2)} . \quad (35)$$

2.3.3 Spectral distribution in the lab frame

The spectral distributions $d\sigma/dE_{4l}$ and $d\sigma/dT_{4l}$ are obtained from the invariant distribution (11) by expressing t and u in terms of E_{4l} , the energy of particle 4 in the lab frame, or in terms of T_{4l} , the kinetic energy. Expanding

$$t = (p_2 - p_4)^2, \quad (36)$$

and noting that in the lab frame $E_2 = m_2$ and $\mathbf{p}_2 = 0$, gives

$$t = m_2^2 + m_4^2 - 2m_2E_{4l} \quad (37)$$

and

$$u = \Sigma m^2 - s - m_2^2 - m_4^2 + 2m_2E_{4l}, \quad (38)$$

with

$$\Sigma m^2 \equiv m_1^2 + m_2^2 + m_3^2 + m_4^2. \quad (39)$$

Both t and u are expressed in terms of T_{4l} by the substitution $E_{4l} = T_{4l} + m_4$, as in

$$t = m_2^2 + m_4^2 - 2m_2(T_{4l} + m_4), \quad (40)$$

$$u = \Sigma m^2 - s - m_2^2 - m_4^2 + 2m_2(T_{4l} + m_4). \quad (41)$$

The range of possible values of E_{4l} and T_{4l} are bound by their minimum and maximum values, which are in turn found by inverting the preceding formulas [10] and substituting t_0 and t_π for t from equation (56), which is listed later in this paper. The above formulas for t and u can now be used to generate $d\sigma/dE_{4l}$ and $d\sigma/dT_{4l}$ from $d\sigma/dt$ and $d\sigma/du$.

2.3.4 Angular distribution in the cm frame

The angular distribution is formed by substituting the expression for \mathcal{M} given by equation (9) [10] and by expressing t and u in terms of angle θ . For a 2 - body final state, this is done by writing the momenta \mathbf{p}_3 and \mathbf{p}_4 in terms of the initial energy in the form of s and λ . The denominator in the direct term in equation (7) contains

$$\begin{aligned} t &\equiv (p_4 - p_2)^2 \\ &= m_4^2 + m_2^2 - 2\sqrt{\mathbf{p}_4^2 + m_4^2}\sqrt{\mathbf{p}_2^2 + m_2^2} + 2|\mathbf{p}_4||\mathbf{p}_2|\cos\theta \\ &= m_4^2 + m_2^2 - 2\sqrt{\mathbf{p}_{f\,cm}^2 + m_4^2}\sqrt{\mathbf{p}_{i\,cm}^2 + m_2^2} + 2|\mathbf{p}_{f\,cm}||\mathbf{p}_{i\,cm}|\cos\theta \quad (\text{cm frame}) \\ &= m_2^2 + m_4^2 + \frac{1}{2s} \left[-\sqrt{(\lambda_{12} + 4sm_2^2)(\lambda_{34} + 4sm_4^2)} + \sqrt{\lambda_{12}\lambda_{34}}\cos\theta \right], \end{aligned} \quad (42)$$

where $\mathbf{p}_{i\,cm} = \mathbf{p}_1 = -\mathbf{p}_2$ and $\mathbf{p}_{f\,cm} = \mathbf{p}_3 = -\mathbf{p}_4$ are the initial and final 3-momenta of the particles in the cm frame. The denominator in the exchange term in equation (8) contains

$$\begin{aligned}
u &\equiv (p_3 - p_2)^2 \\
&= m_3^2 + m_2^2 - 2E_3E_2 + 2\mathbf{p}_3 \cdot \mathbf{p}_2 \\
&= m_3^2 + m_2^2 - 2E_3E_2 - 2\mathbf{p}_4 \cdot \mathbf{p}_2 && \text{(because } \mathbf{p}_3 + \mathbf{p}_4 = 0 \text{ in cm frame)} \\
&= m_3^2 + m_2^2 - 2\sqrt{\mathbf{p}_4^2 + m_3^2}\sqrt{\mathbf{p}_2^2 + m_2^2} - 2|\mathbf{p}_4||\mathbf{p}_2|\cos\theta && \text{(in cm frame)} \\
&= m_3^2 + m_2^2 - 2\sqrt{\mathbf{p}_{f\,cm}^2 + m_3^2}\sqrt{\mathbf{p}_{i\,cm}^2 + m_2^2} - 2|\mathbf{p}_{f\,cm}||\mathbf{p}_{i\,cm}|\cos\theta && \text{(in cm frame)} \\
&\equiv \Sigma m^2 - s - t, && (43)
\end{aligned}$$

where θ is the angle between \mathbf{p}_2 and \mathbf{p}_4 in the cm frame. The angular distribution becomes [10]

$$\begin{aligned}
\left(\frac{d\sigma}{d\Omega_4}\right)_{cm} &= \frac{\mathcal{S}}{64\pi^2s} \sqrt{\frac{\lambda_{34}}{\lambda_{12}}} |\mathcal{M}|^2 \\
&= \frac{\mathcal{S}}{64\pi^2s} \sqrt{\frac{\lambda_{34}}{\lambda_{12}}} \left[\frac{g_{12x}g_{34x}}{t - m_x^2} + \frac{g_{12x}g_{34x}}{u - m_x^2} \right]^2, && (44)
\end{aligned}$$

with the definitions

$$t \equiv m_2^2 + m_4^2 + \frac{1}{2s} \left[-\sqrt{(\lambda_{12} + 4sm_2^2)(\lambda_{34} + 4sm_4^2)} + \sqrt{\lambda_{12}\lambda_{34}} \cos\theta \right], \quad (45)$$

and

$$u \equiv \Sigma m^2 - s - t. \quad (46)$$

In the cm frame, the angular distributions of particles 3 and 4 are equivalent [10].

$$d\sigma/d\Omega_{3c} \equiv d\sigma/d\Omega_{4c}. \quad (47)$$

Comparing equation (11) with equations (44) and (45), the differential cross sections take a simpler form when written in terms of the Mandelstam variables s , t and u , instead of the momentum $|\mathbf{p}|$ and angle θ .

2.3.5 Angular distribution in the lab frame

The angular distribution in the lab frame may be expressed in terms of the angular distribution in the cm frame [10],

$$\begin{aligned}
\frac{d\sigma}{d\Omega_{3l}} &= \frac{4m_2s}{\sqrt{\lambda_{12}\lambda_{34}}} \frac{|\mathbf{p}_{1l}||\mathbf{p}_{3l}|}{|E_{1l} + m_2 - \frac{|\mathbf{p}_{1l}|}{|\mathbf{p}_{3l}|}E_{3l}\cos\theta_{13l}|} \frac{d\sigma}{d\Omega_{13c}} \\
&= \frac{4m_2s}{\sqrt{\lambda_{12}\lambda_{34}}} \frac{2\sqrt{E_{1l}^2 - m_1^2} (E_{3l}^2 - m_3^2)^{3/2}}{|E_{3l}(m_1^2 + m_2^2 + m_3^2 - m_4^2 + 2E_1m_2) - 2m_3^2(E_1 + m_2)|} \frac{d\sigma}{d\Omega_{13c}}. && (48)
\end{aligned}$$

For computational purposes, both E_{3l} and $d\sigma/d\Omega_{13c}$, which contain t , may be written as functions of θ_{13l} and the energy of particle 1 in the lab frame E_{1l} (instead of s), by using the following relations for $s(E_{1l})$ and $t(E_{1l}, \theta_{3l})$,

$$s(E_{1l}) = m_1^2 + m_2^2 + 2E_{1l}m_2, \quad (49)$$

and

$$t(E_{1l}, \theta_{3l}) = m_4^2 - m_2^2 + 2m_2[E_3(E_{1l}, \theta_{3l}) - E_{1l}]. \quad (50)$$

The expression for s is found by expanding $s = (p_{1l} + p_{2l})^2$ and noting that in the lab frame $\mathbf{p}_2 = 0$ and $E_{2l} = m_2$. The expression for t is found, following reference [10], by expanding $t = (p_2 - p_4)^2$ and eliminating E_{4l} using conservation of energy, $E_{4l} = E_{1l} + m_2 - E_{3l}$. Then [10]

$$E_{3l}(E_{1l}, \theta_{3l}) = \frac{ab \pm \sqrt{E_{1l}^2 - m_1^2} \cos(\theta_{3l}) \sqrt{a^2 - m_3^2 [b^2 - (E_{1l}^2 - m_1^2) \cos^2(\theta_{3l})]}}{b^2 - (E_{1l}^2 - m_1^2) \cos^2(\theta_{3l})}, \quad (51)$$

where

$$a = \frac{s + m_3^2 - m_4^2}{2}, \quad (52)$$

and

$$b = E_{1l} + m_2. \quad (53)$$

Note the double valued nature of the energy expression (51). A discussion of how to handle this in computations is discussed in reference [10].

2.3.6 Singularities

The differential cross sections in equations (16), (17), and (18) have singularities at

$$t = m^2, \quad (54)$$

and

$$u = m^2, \quad (55)$$

where $m \equiv m_x$. In this section, we show that these singularities are never encountered for physical values of t and u . The formulas derived in reference [10] for the extreme values of t denoted as $t_0 = t(\theta = 0)$ and $t_\pi = t(\theta = \pi)$, are

$$t_0(t_\pi) = \frac{1}{4s} \left[(m_1^2 - m_2^2 - m_3^2 + m_4^2)^2 - (\sqrt{\lambda_{12}} \mp \sqrt{\lambda_{34}})^2 \right]. \quad (56)$$

The symbol \mp means that a negative sign is used for t_0 and a positive sign is used for t_π . A useful result is the following equation.

$$u_0 - t_\pi = u_\pi - t_0 = \frac{1}{s} (m_1^2 - m_2^2)(m_3^2 - m_4^2). \quad (57)$$

Thus, for the reaction $NN \rightarrow \text{anything}$, we have

$$u_0 = t_\pi, \quad (58)$$

$$u_\pi = t_0. \quad (59)$$

We now consider the two cases of elastic and inelastic scattering.

Elastic scattering (e.g. $NN \rightarrow NN$)

For the case of $m_1 = m_2 = m_3 = m_4 \equiv m_N$, the threshold value of s , denoted s_t is

$$s_t = 4m_N^2. \quad (60)$$

The equal masses case gives

$$\lambda_{12} = \lambda_{34} = s(s - s_t) = s(s - 4m_N^2). \quad (61)$$

By equation (56),

$$t_0 = 0 \quad (62)$$

and

$$t_\pi = s_t - s = 4m_N^2 - s. \quad (63)$$

Clearly, t_0 has a fixed value, but the value of t_π depends on s . The minimum value of s is $s_t = 4m_N^2$ and so the minimum and maximum values of t_π are

$$t_\pi^{\min}(s \rightarrow \infty) = -\infty \quad (64)$$

and

$$t_\pi^{\max}(s = s_t) = 0, \quad (65)$$

and so the range of t_π is

$$t_\pi : -\infty \rightarrow 0. \quad (66)$$

Clearly, the singularity value $t = m^2$ is never encountered when t ranges between t_0 and t_π . Now, consider the singularity at $u = m^2$, where $s + t + u = m_1^2 + m_2^2 + m_3^2 + m_4^2 = 4m_N^2 = s_t$. Thus, $u = 4m_N^2 - s - t = s_t - s - t$. The extremum values of u can be obtained with equation (59). Thus, the extremum values of u are the (opposite) extremum values of t . Given that the singularity value $t = m^2$ is never encountered when t ranges between t_0 and t_π , it follows that the singularity value $u = m^2$ is never encountered when u ranges between u_0 and u_π .

Inelastic scattering (e.g. $NN \rightarrow N\Delta$)

For the case of $m_1 = m_2 = m_3 \equiv m_N$ and $m_4 \equiv m_\Delta$, the threshold value of s , denoted s_t is

$$s_t = (m_N + m_\Delta)^2 \quad (67)$$

and

$$\lambda_{12} = s(s - 4m_N^2) \quad (\text{same as elastic case}) \quad (68)$$

and

$$\lambda_{34} = (s - m_N^2 - m_\Delta^2)^2 - 4m_N^2 m_\Delta^2. \quad (69)$$

One uses equation (56) to obtain

$$t_0(t_\pi) = \frac{1}{2s} \left[s(m_\Delta^2 + 3m_N^2 - s) \pm \sqrt{s(s - 4m_N^2)} \sqrt{(s - m_N^2 - m_\Delta^2)^2 - 4m_N^2 m_\Delta^2} \right] \quad (70)$$

The symbol \pm means that a $+$ sign is used for t_0 and a $-$ sign is used for t_π . The minimum and maximum values of t_0 are

$$t_0^{\min}(s = s_t) = m_N(m_N - m_\Delta) \quad (71)$$

and

$$t_0^{\max}(s \rightarrow \infty) = 0, \quad (72)$$

giving the range of t_0 as

$$t_0 : m_N(m_N - m_\Delta) \rightarrow 0. \quad (73)$$

Note that if we had m_N in place of m_Δ , these results reduce to equation (62). The minimum and maximum values of t_π are

$$t_\pi^{\min}(s \rightarrow \infty) = -\infty \quad (74)$$

and

$$t_\pi^{\max}(s = s_t) = m_N(m_N - m_\Delta) = t_0^{\min}, \quad (75)$$

giving the range of t_π as

$$t_\pi : -\infty \rightarrow m_N(m_N - m_\Delta). \quad (76)$$

If we had m_N in place of m_Δ , these results reduce to equations (64), (65), and (66). Clearly, the singularity value $t = m^2$ is never encountered when t ranges between t_0 and t_π .

Now consider the singularity at $u = m^2$. The extremum values of u can be obtained with equation (59). Thus, the extremum values of u are the (opposite) extremum values of t . Given that the singularity value $t = m^2$ is never encountered when t ranges between t_0 and t_π , then the singularity value $u = m^2$ is never encountered when u ranges between u_0 and u_π .

2.4 Scattering via zero-mass exchange particle

In this section, we consider scattering by means of an exchange particle with mass $m = 0$. By setting the coupling constant $g = g_{\gamma NN} = \alpha \simeq 1/137$, the exchange particle becomes the photon, except that in keeping with the scalar model, the photon is treated not as a spin 1 particle, but as a scalar. In the next section, both the elastic $NN \rightarrow NN$ (Rutherford) and inelastic $NN \rightarrow N\Delta$ cases are examined numerically. The formalism developed in the preceding sections gives the well known differential cross section for Rutherford scattering, which is characterized by $g_{13x} = g_{24x} \equiv g$, the exchange particle mass $m_x = 0$, and in the general case $m_1 = m_3$ and $m_2 = m_4$ (i.e. elastic scattering). In our special case, for simplicity we make the further restriction $m_1 = m_2 \equiv M$, so that, in the cm frame, $|\mathbf{p}_1| = |\mathbf{p}_2| = |\mathbf{p}_3| = |\mathbf{p}_4| \equiv |\mathbf{p}_{cm}| \equiv |\mathbf{p}|$. Also, $E_1 = E_2 = E_3 = E_4 \equiv E$. Thus,

$$\begin{aligned}
t \equiv (p_4 - p_2)^2 &= m_4^2 + m_2^2 - 2E_4E_2 + 2\mathbf{p}_4 \cdot \mathbf{p}_2 \\
&= 2M^2 - 2E^2 + 2\mathbf{p}^2 \cos \theta \\
&= 2(-\mathbf{p}^2 + \mathbf{p}^2 \cos \theta) = -2\mathbf{p}^2(1 - \cos \theta) \\
&= -\frac{\lambda}{2s}(1 - \cos \theta) ,
\end{aligned} \tag{77}$$

where, by equation (12),

$$\lambda \equiv \lambda(s, M^2, M^2) = s(s - 4M^2) = 4s\mathbf{p}^2 . \tag{78}$$

Also,

$$\begin{aligned}
u \equiv (p_3 - p_2)^2 &= m_3^2 + m_2^2 - 2E_3E_2 + 2\mathbf{p}_3 \cdot \mathbf{p}_2 \\
&= m_3^2 + m_2^2 - 2E_3E_2 - 2\mathbf{p}_4 \cdot \mathbf{p}_2 \\
&= -\frac{\lambda}{2s}(1 + \cos \theta) .
\end{aligned} \tag{79}$$

Thus, by equation (9), the invariant amplitude, with $m_x = 0$, is

$$\begin{aligned}
\mathcal{M} = -g^2 \left[\frac{1}{t} + \frac{1}{u} \right] &= -g^2 \left[\frac{1}{(p_4 - p_2)^2} + \frac{1}{(p_3 - p_2)^2} \right] \\
&= \frac{2sg^2}{\lambda} \left(\frac{1}{1 - \cos \theta} + \frac{1}{1 + \cos \theta} \right) \\
&= \frac{4sg^2}{\lambda \sin^2 \theta} \\
&= \frac{4g^2}{(s - 4M^2) \sin^2 \theta} .
\end{aligned} \tag{80}$$

Equation (44) becomes

$$\frac{d\sigma}{d\Omega_{cm}} = \frac{\mathcal{S}}{64\pi^2 s} |\mathcal{M}|^2 = \frac{\mathcal{S}}{64\pi^2 s} \frac{16g^4}{(s - 4M^2)^2 \sin^4 \theta} , \tag{81}$$

giving the Rutherford formula (with $\mathcal{S} = 1/2!$) as

$$\frac{d\sigma}{d\Omega_{cm}} = \frac{\mathcal{S}}{64\pi^2 s} |\mathcal{M}|^2 = \frac{g^4}{8\pi^2 s (s - 4M^2)^2 \sin^4 \theta}. \quad (82)$$

This agrees with Griffiths [7] (equation 6.54), as can be seen using $s = 4E^2$ and $\mathbf{p}^2 = \frac{\lambda}{4s} = \frac{s(s-4M^2)}{4s} = \frac{1}{4}(s-4M^2)$. The classical and quantum mechanical results for $d\sigma/d\Omega$ exhibit several differences (compare Griffiths [7] equation 6.54 with p. 194). The classical result for Rutherford scattering typically encountered (e.g. Griffiths [7] (p. 194), or Goldstein [11] (equation 3.102)) depends on $\theta/2$ rather than θ . This difference of a factor of 2 is due to the fact that the classical calculation is usually performed in the lab (target) frame, whereas the present calculation is performed in the cm frame. In the non-relativistic limit, for the case of all particles having the same mass, we have precisely $\theta_{lab} \equiv \theta_{cm}/2$. See Marion [12] (equation 9.71).

The classical and quantum mechanical results for $d\sigma/d\Omega$ also differ by an overall factor of 2. This well known difference arises from the quantum mechanical description of a particle as a wave packet, versus the classical description of particles as having finite extent (see Bohm [13] sections 17 and 49 for a discussion). As expected, the Rutherford formula diverges at $s = 0$ and $s = 4M^2$, just as the formula of Griffiths [7] which diverges at $E = 0$ or $\mathbf{p}^2 = 0$. Since $s \equiv (p_1 + p_2)^2$, the value of s in the cm frame is $s = (E_1 + E_2)^2$, which has a minimum value at $s = 4M^2$ for $m_1 = m_2 \equiv M$. Thus, the singularity at $s = 4M^2$ is the same as the singularity at $\mathbf{p}^2 = 0$. As for the case $s = 0$, this value is never reached because the minimum value of s is $4M^2$. Similarly, the value $E = 0$ is never reached because the minimum value of E is M . As mentioned in the previous section, the equation for the angular distribution is much simpler if Mandelstam variables are used instead of angle,

$$\frac{d\sigma}{d\Omega_{cm}} = \frac{\mathcal{S}g^4}{64\pi^2 s} \left(\frac{1}{t} + \frac{1}{u}\right)^2, \quad (83)$$

with $u = 4M^2 - s - t$.

2.5 Total cross section

In this subsection the previous differential cross sections will be integrated to form total cross sections. The total cross sections are obtained by integrating [10]

$$\sigma = \int_{t_\pi}^{t_0} dt \frac{d\sigma}{dt} \quad (84)$$

or

$$\sigma = \int_{u_0}^{u_\pi} du \frac{d\sigma}{du}. \quad (85)$$

The expressions for the direct, exchange, and interference t distributions were given in equations (16), (17) and (18). The total cross sections can be obtained with straightforward analytic integration. The direct cross section is

$$\sigma_d = \int_{t_\pi}^{t_0} dt \frac{K}{(t - m^2)^2} = -K \left[\frac{1}{t - m^2} \right]_{t_\pi}^{t_0}, \quad (86)$$

giving

$$\sigma_d = K \left(\frac{1}{t_\pi - m^2} - \frac{1}{t_0 - m^2} \right). \quad (87)$$

The exchange cross section is

$$\begin{aligned} \sigma_e &= \int_{t_\pi}^{t_0} dt \frac{K}{(u - m^2)^2} \\ &= \int_{t_\pi}^{t_0} dt \frac{K}{(\Sigma m^2 - s - t - m^2)^2} = \int_{t_\pi}^{t_0} dt \frac{K}{(t + s - \Sigma m^2 + m^2)^2} \\ &= -K \left[\frac{1}{t + s - \Sigma m^2 + m^2} \right]_{t_\pi}^{t_0} \\ &= K \left(\frac{1}{t_\pi + s - \Sigma m^2 + m^2} - \frac{1}{t_0 + s - \Sigma m^2 + m^2} \right) \\ &= K \left(\frac{1}{t_\pi - m^2} - \frac{1}{t_0 - m^2} \right), \end{aligned} \quad (88)$$

giving

$$\sigma_e = \sigma_d. \quad (89)$$

Thus, the direct and exchange total cross sections are equal. Note that this result is more easily obtained by direct integration of the u variable. Since $du = -dt$, and using (59), we have

$$\begin{aligned} \sigma_e &= \int_{u_0}^{u_\pi} du \frac{K}{(u - m^2)^2} \\ &= \int_{t_\pi}^{t_0} dt \frac{K}{(u - m^2)^2} \\ &= \sigma_d \end{aligned} \quad (90)$$

Now consider integration of the interference term given in equation (18).

$$\begin{aligned} \frac{d\sigma_i}{dt} &= \frac{2K}{(t - m^2)(u - m^2)} = \frac{2K}{(t - m^2)(-t + \Sigma m^2 - s - m^2)} \\ &= \frac{2K}{-t^2 + t(\Sigma m^2 - s) + m^2(s - \Sigma m^2 + m^2)}. \end{aligned} \quad (91)$$

The needed integral is of the form [14]

$$\begin{aligned} \int \frac{dx}{ax^2 + bx + c} &= \frac{2}{\sqrt{4ac - b^2}} \tan^{-1} \left(\frac{2ax + b}{\sqrt{4ac - b^2}} \right), & \text{for } b^2 - 4ac < 0, \\ &= \frac{1}{\sqrt{b^2 - 4ac}} \log \left(\frac{2ax + b - \sqrt{b^2 - 4ac}}{2ax + b + \sqrt{b^2 - 4ac}} \right), & \text{for } b^2 - 4ac > 0, \\ &= \frac{-1}{ax + \frac{1}{2}b}, & \text{for } b^2 - 4ac = 0. \end{aligned} \quad (92)$$

Note that if $b = 0$, the result of equation (92) reduces to the correct form for both cases of the \tan^{-1} or \log . However, if $a = 0$ or $c = 0$, the result of equation (92) does not reduce to the correct form. In fact, for $a = 0$, we have [14]

$$\int \frac{dx}{bx + c} = \frac{1}{b} \log(bx + c) , \quad (93)$$

and for $c = 0$ we have [14]

$$\int \frac{dx}{ax^2 + bx} = \frac{1}{b} \log\left(\frac{x}{ax + b}\right) . \quad (94)$$

For our case, we have

$$a = -1 \quad b = \Sigma m^2 - s \quad c = m^2(s - \Sigma m^2 + m^2) , \quad (95)$$

and we never come across the situation where $a = 0$ or $c = 0$. The minimum value of c occurs at $s = s_{\text{threshold}} = (m_3 + m_4)^2$. Thus,

$$\begin{aligned} c_{\min} &= m^2[(m_3 + m_4)^2 - m_1^2 - m_2^2 - m_3^2 - m_4^2 + m^2] \\ &= m^2 - (m_1 - m_2)^2 + 2(m_3 m_4 - m_1 m_2) , \end{aligned} \quad (96)$$

but since we always have $m_3 m_4 \geq m_1 m_2$, then

$$c_{\min} \geq m^2 - (m_1 - m_2)^2 , \quad (97)$$

giving

$$m = m_\pi > |m_1 - m_2| \Rightarrow c > 0 . \quad (98)$$

Thus, we can conceivably run across the case where $c = 0$. Now we can have $b = 0$ at $s = \Sigma m^2$ but that is no problem because, in that case, the integral above reduces to the correct form. Given that the result depends on the value of $b^2 - 4ac$, we need to evaluate this quantity for the expression in equation (91), with the result that

$$b^2 - 4ac = (\Sigma m^2 - s)^2 + 4m^2(s - \Sigma m^2 + m^2) . \quad (99)$$

Define $\bar{s} \equiv s - \Sigma m^2 + m^2$ so that $s - \Sigma m^2 = \bar{s} - m^2$, to give

$$\begin{aligned} b^2 - 4ac &= (\bar{s} - m^2)^2 + 4m^2 \bar{s} = \bar{s}^2 + 2m^2 \bar{s} + m^4 , \\ &= (\bar{s} + m^2)^2 \end{aligned} \quad (100)$$

which finally gives

$$b^2 - 4ac = (s - \Sigma m^2 + 2m^2)^2 , \quad (101)$$

which, being a square, always gives

$$b^2 - 4ac \geq 0 . \quad (102)$$

Following a similar analysis for c above we have

$$\begin{aligned} (b^2 - 4ac)_{\min} &= [(m_3 + m_4)^2 - m_1^2 - m_2^2 - m_3^2 - m_4^2 + 2m^2]^2 \\ &= [2m^2 - (m_1 - m_2)^2 + 2(m_3m_4 - m_1m_2)]^2, \end{aligned} \quad (103)$$

but since we always have $m_3m_4 \geq m_1m_2$, then

$$(b^2 - 4ac)_{\min} \geq [2m^2 - (m_1 - m_2)^2]^2, \quad (104)$$

giving

$$\sqrt{2} m > |m_1 - m_2| \Rightarrow b^2 - 4ac \geq 0. \quad (105)$$

Thus, we can conceivably run across the case where $b^2 - 4ac = 0$. The following analysis assumes that $c \neq 0$ and $b^2 - 4ac \neq 0$. The total interference cross section is given by

$$\begin{aligned} \sigma_i &= \int_{t_\pi}^{t_0} dt \frac{2K}{-t^2 + t(\Sigma m^2 - s) + m^2(s - \Sigma m^2 + m^2)} \\ &= \frac{2K}{s - \Sigma m^2 + 2m^2} \left[\log \frac{t + s - \Sigma m^2 + m^2}{t - m^2} \right]_{t_\pi}^{t_0}, \end{aligned} \quad (106)$$

which becomes

$$\sigma_i = \frac{2K}{s - \Sigma m^2 + 2m^2} \left[\log \frac{(t_\pi - m^2)(t_0 + s - \Sigma m^2 + m^2)}{(t_0 - m^2)(t_\pi + s - \Sigma m^2 + m^2)} \right]. \quad (107)$$

Elastic scattering (e.g. $NN \rightarrow NN$)

For the reaction $NN \rightarrow NN$, we obtain

$$t_0 = 0, \quad (108)$$

$$t_\pi = 4m_N^2 - s, \quad (109)$$

which, upon substitution into equation (87), gives

$$\begin{aligned} \sigma_d &= K \left(\frac{1}{m^2} - \frac{1}{s - 4m_N^2 + m^2} \right) \\ &= \frac{g_{\pi NN}^4}{32\pi s(s - 4m_N^2)} \left(\frac{1}{m^2} - \frac{1}{s - 4m_N^2 + m^2} \right), \end{aligned} \quad (110)$$

which simplifies to

$$\sigma_d = \frac{g_{\pi NN}^4}{32\pi m^2 s(s - 4m_N^2 + m^2)}. \quad (111)$$

Note that the minimum value of s is $s_t \equiv s_{\text{threshold}} = (m_3 + m_4)^2 = 4m_N^2$ and so the cross section has no singularities. The largest value of σ occurs at $s = s_t$.

$$\begin{aligned}
\sigma_d(s \rightarrow s_t) &= \frac{g_{\pi NN}^4}{32\pi m_\pi^4 s_t} = \frac{g_{\pi NN}^4}{128\pi m_\pi^4 m_N^2} \\
&= \frac{1}{8\pi m_N^2} \left(\frac{g_{\pi NN}}{2m_\pi} \right)^4 \\
&= \frac{\mathcal{S}}{4\pi m_N^2} \left(\frac{g_{\pi NN}}{2m_\pi} \right)^4.
\end{aligned} \tag{112}$$

The other important limit is

$$\sigma_d(s \rightarrow \infty) = 0. \tag{113}$$

Recall (89), which showed that the direct and exchange total cross sections are the same. The sum of direct and exchange maximum values is

$$\begin{aligned}
\sigma_d^{\text{max}} + \sigma_e^{\text{max}} &= \frac{2\mathcal{S}}{4\pi m_N^2} \left(\frac{g_{\pi NN}}{2m_\pi} \right)^4 \\
&= \frac{1}{4\pi m_N^2} \left(\frac{g_{\pi NN}}{2m_\pi} \right)^4.
\end{aligned} \tag{114}$$

The interference cross section is given by substitution into equation (107),

$$\begin{aligned}
\sigma_i &= \frac{2K}{s - 4m_N^2 + 2m_\pi^2} \log \left[\frac{(4m_N^2 - s - m_\pi^2)(s - 4m_N^2 + m_\pi^2)}{-m_\pi^2(4m_N^2 - s + s - 4m_N^2 + m_\pi^2)} \right] \\
&= \frac{4K}{s - 4m_N^2 + 2m_\pi^2} \log \left(\frac{s - 4m_N^2 + m_\pi^2}{m_\pi^2} \right),
\end{aligned} \tag{115}$$

which is

$$\begin{aligned}
\sigma_i &= \frac{g_{\pi NN}^4}{8\pi s(s - 4m_N^2)(s - 4m_N^2 + 2m_\pi^2)} \log \frac{s - 4m_N^2 + m_\pi^2}{m_\pi^2} \\
&= 4\sigma_d m^2 \frac{s - 4m_N^2 + m_\pi^2}{s - 4m_N^2 + 2m_\pi^2} \frac{1}{s - 4m_N^2} \log \frac{s - 4m_N^2 + m_\pi^2}{m_\pi^2}.
\end{aligned} \tag{116}$$

This cross section has a potential threshold singularity at $s = s_t = 4m_N^2$, which comes from the term $K \equiv K(s) \equiv \frac{\mathcal{S}}{16\pi\lambda_{12}} g_{13x}^2 g_{24x}^2 = \frac{g_{\pi NN}^4}{32\pi s(s - 4m_N^2)}$. The singularity was canceled out in our previous expression for σ_d in equations (110) and (111). Clearly, we need to evaluate the term

$\frac{1}{(s-s_t)} \log \frac{s-s_t+m^2}{m^2}$ near $s = s_t$. Consider the following Taylor series expansion [14] (p. 111)

$$\begin{aligned}
\frac{1}{(s-s_t)} \log \left(\frac{s-s_t+m^2}{m^2} \right) &= \frac{1}{(s-s_t)} \log \left(\frac{s-s_t}{m^2} + 1 \right) \\
&= \frac{1}{m^2 x} \log(1+x) \quad \text{with } x \equiv \frac{s-s_t}{m^2} \\
&= \frac{1}{m^2 x} \left(x - \frac{x^2}{2} + \frac{x^3}{3} - \frac{x^4}{4} + \dots \right) \\
&= \frac{1}{m^2} \left(1 - \frac{x}{2} + \frac{x^2}{3} - \frac{x^3}{4} + \dots \right), \tag{117}
\end{aligned}$$

which gives

$$\lim_{s \rightarrow s_t} \frac{1}{(s-s_t)} \log \left(\frac{s-s_t+m^2}{m^2} \right) = \frac{1}{m^2}. \tag{118}$$

Substituting into the above expression gives the interference cross section at threshold $s = s_t$,

$$\begin{aligned}
\sigma_i^{\max} = \sigma_i(s \rightarrow s_t) &= 2\sigma_d^{\max} \\
&= \sigma_d^{\max} + \sigma_e^{\max}, \tag{119}
\end{aligned}$$

which is an interesting result because it shows that *in the low energy limit, the interference term dominates*. The other important limit is

$$\sigma_i(s \rightarrow \infty) = 0. \tag{120}$$

Inelastic scattering (e.g. $NN \rightarrow N\Delta$)

For the $NN \rightarrow N\Delta$ reaction, we obtain from equation (56)

$$t_0(t_\pi) = \frac{1}{2s} \left[s(m_\Delta^2 + 3m_N^2 - s) \pm \sqrt{s(s-4m_N^2)} \sqrt{(m_\Delta^2 + m_N^2 - s)^2 - 4m_N^2 m_\Delta^2} \right]. \tag{121}$$

Substituting gives

$$\sigma_d = \frac{g_{\pi NN}^2 g_{\pi N\Delta}^2 \sqrt{(s-m_\Delta^2 - m_N^2)^2 - 4m_\Delta^2 m_N^2}}{16\pi \sqrt{s(s-4m_N^2)} [s^2 m^2 + s m^2 (m^2 - m_\Delta^2 - 3m_N^2) + (m_N^3 - m_\Delta^2 m_N)^2]}, \tag{122}$$

and

$$\begin{aligned}
\sigma_i &= \frac{g_{\pi NN}^2 g_{\pi N\Delta}^2}{4\pi s (s-4m_N^2) (s+2m^2 - m_\Delta^2 - 3m_N^2)} \\
&\times \log \left[\frac{s(s+2m^2 - m_\Delta^2 - 3m_N^2) + \sqrt{s(s-4m_N^2)} \sqrt{(s-m_\Delta^2 - m_N^2)^2 - 4m_\Delta^2 m_N^2}}{s(s+2m^2 - m_\Delta^2 - 3m_N^2) - \sqrt{s(s-4m_N^2)} \sqrt{(s-m_\Delta^2 - m_N^2)^2 - 4m_\Delta^2 m_N^2}} \right]. \tag{123}
\end{aligned}$$

Note that if one replaces the Δ mass with the nucleon mass, these results reduce to the elastic formulas obtained previously (except for the statistical factor \mathcal{S}). Also note the following limits.

$$\sigma_d(s \rightarrow s_{\text{threshold}}) = \sigma_d(s \rightarrow \infty) = 0 , \quad (124)$$

$$\sigma_i(s \rightarrow s_{\text{threshold}}) = \sigma_i(s \rightarrow \infty) = 0 . \quad (125)$$

2.5.1 Asymptotic region

We now consider a theoretical check of our cross section result. The Froissart theorem [15] (p. 344) states that in the high energy limit $s \rightarrow \infty$, the total cross section of an arbitrary collision process is bounded by

$$\sigma_{tot} < \text{Constant} \times [\log s]^2 . \quad (126)$$

For the elastic $pp \rightarrow pp$ and inelastic processes $pp \rightarrow p\Delta^+$, allowing s to become large leads to equations (113), (120), (124) and (125), which shows that the total cross sections predicted by the scalar OPE model go to zero in the high energy limit, in agreement with the theorem.

3 Calculations for 2 - body final states

The previous section developed the basic theory for calculating 2 - body final state cross sections. In the present section, these cross section formulas are illustrated with numerical results and plots for the scattering processes $pp \rightarrow pp$ and $pp \rightarrow p\Delta$, and the decay $\Delta \rightarrow p\pi^0$.

3.1 Coupling constants

In this subsection, some comments will be made about coupling constants. In quantum field theories, the coupling “constants” are in fact not constants, but depend on the momentum p of the interaction, thus $g_{\pi NN} = g_{\pi NN}(p)$ [7] (p. 62), [16] (pp. 146 - 151). From the perspective of the quark model, $g_{\pi NN}$ hides the underlying quark-gluon interactions, whose strengths are a function of the momentum of the quark-gluon interactions. The low energy pion-nucleon coupling constant $g_{\pi NN}$ has been experimentally determined to be [17]

$$g_{\pi NN}^2/4\pi \approx 14 , \quad (127)$$

for the coupling of neutral pions to protons and neutrons. The coupling of charged pions is a factor $\sqrt{2}$ stronger [18] (p. 184); [19] (p. 219). In quantum field theories where spin is taken into account, the coupling constants are dimensionless. However, in the scalar OPE theory the coupling constants must have dimensions of GeV [7] (p. 202).

3.2 Calculations for scattering involving a massive exchange particle

The exchange particle is always either massive or massless, and quite different behaviors in cross sections arise as a result. In this subsection, we give results for massive particle exchange.

3.2.1 Minimum and maximum values of t

Consider the reactions $pp \rightarrow pp$ and $pp \rightarrow p\Delta^+$. We ignore the particle spins and assume that the exchange particle is a neutral pion in both cases. This is consistent with the use of a scalar theory, in that other pion isospin states are not included. Also, the use of a single pion exchange, as opposed to multiple exchanges, is an approximation expected to be valid at low energy. At higher energy, multiple exchanges can be introduced, or parameters, such as coupling constants, can be adjusted to fit data. Using the following particle masses $m_p = 938.27$ MeV, $m_x = m_{\pi^0} = 134.98$ MeV, $m_{\Delta^+} = 1232$ MeV, we wish to calculate the value of $\frac{d\sigma}{dt}$, in units of mb/GeV² for both reactions at $s = 2s_{\text{threshold}}$ (twice the threshold to produce the Δ) for the maximum and minimum values of t given by (56)

$$t_0(t_\pi) = \frac{1}{4s} \left[(m_1^2 - m_2^2 - m_3^2 + m_4^2)^2 - (\sqrt{\lambda_{12}} - (+)\sqrt{\lambda_{34}})^2 \right]. \quad (128)$$

The notation t_π is bound to be a little confusing given the the particle we are talking about is the pion with symbol π . The symbol t_π refers to the value of the t variable at the angle of π radians. We obtain the following results. For the reaction $pp \rightarrow pp$, we calculate the following results.

$$s_{\text{threshold}} = 3.52 \text{ GeV}^2, \quad (129)$$

$$t_0(2s_{\text{threshold}}) = 0 \text{ GeV}^2, \quad (130)$$

$$t_\pi(2s_{\text{threshold}}) = -3.52 \text{ GeV}^2, \quad (131)$$

$$\frac{d\sigma}{dt}(s = 2s_{\text{threshold}}, t = t_0) = 14700 \frac{\text{mb}}{\text{GeV}^2}, \quad (132)$$

$$\frac{d\sigma}{dt}(s = 2s_{\text{threshold}}, t = t_\pi) = 14700 \frac{\text{mb}}{\text{GeV}^2}. \quad (133)$$

For the reaction $pp \rightarrow p\Delta^+$, we calculate the following results.

$$s_{\text{threshold}} = 4.71 \text{ GeV}^2, \quad (134)$$

$$t_0(2s_{\text{threshold}}) = -0.00723 \text{ GeV}^2, \quad (135)$$

$$t_\pi(2s_{\text{threshold}}) = -5.25 \text{ GeV}^2, \quad (136)$$

$$\frac{d\sigma}{dt}(s = 2s_{\text{threshold}}, t = t_0) = 6720 \frac{\text{mb}}{\text{GeV}^2}, \quad (137)$$

$$\frac{d\sigma}{dt}(s = 2s_{\text{threshold}}, t = t_\pi) = 6720 \frac{\text{mb}}{\text{GeV}^2}. \quad (138)$$

The cross sections are the same at the values of t_0 and t_π because the center of momentum frame does not distinguish forward and backward scattering.

3.2.2 Singularities

The invariant amplitude \mathcal{M} in equation (9) has singularities at $t = m_x^2$ and $u = m_x^2$. These singularities are not encountered for the reactions considered above. To show this, we evaluate t at the singularities and compare to the values of t_0 and t_π for the case of $s = 2s_{\text{threshold}}$.

Results for the reaction $pp \rightarrow pp$ are

$$s_{\text{threshold}} = 3.5214 \text{ GeV}^2 \quad (139)$$

$$t_0(2s_{\text{threshold}}) = 0 \text{ GeV}^2 \quad (140)$$

$$t_\pi(2s_{\text{threshold}}) = -3.5214 \text{ GeV}^2. \quad (141)$$

The t singularity occurs at

$$t = m_x^2 = 0.0182196 \text{ GeV}^2. \quad (142)$$

The u singularity occurs at

$$u = m_1^2 + m_2^2 + m_3^2 + m_4^2 - m_x^2 - s - t = -3.53962 \text{ GeV}^2. \quad (143)$$

For these maximum and minimum values of t (t_0 and t_π), the singularities are never encountered.

Results for the reaction $pp \rightarrow p\Delta^+$ are

$$s_{\text{threshold}} = 4.71007 \text{ GeV}^2, \quad (144)$$

$$t_0(2s_{\text{threshold}}) = -0.00722818 \text{ GeV}^2, \quad (145)$$

$$t_\pi(2s_{\text{threshold}}) = -5.25404 \text{ GeV}^2. \quad (146)$$

The t singularity occurs at

$$t = m_x^2 = 0.0182196 \text{ GeV}^2. \quad (147)$$

The u singularity occurs at

$$u = m_1^2 + m_2^2 + m_3^2 + m_4^2 - m_x^2 - s - t = -5.27949 \text{ GeV}^2. \quad (148)$$

For these maximum and minimum values of t (i.e. t_0 and t_π), the singularities are never encountered.

3.3 Invariant distribution $d\sigma/dt$

The Lorentz invariant differential cross section $d\sigma/dt$ is very useful because it represents the complicated, non-invariant angular distribution in a very simple way. This subsection develops explicit formulas for this invariant cross section. Equation (11) is used to calculate the invariant distribution $d\sigma/dt$. The total cross section σ is determined by integrating $d\sigma/dt$ over the range $t = [t_0, t_\pi]$, with t_0 and t_π given by (56). The exchange particle is the π^0 . By setting the mass $m_4 = m_\Delta$, the mass of the Δ particle, we generate results for the reaction $pp \rightarrow p\Delta^+$. For the reaction $pp \rightarrow pp$, results are obtained by setting $m_4 = m_p$, the mass of the proton. Figure 4 plots $d\sigma/dt$ at $s = 2s_{\text{threshold}}$. The shape of the plot agrees with Reference [20] (figure 4.8). The t and u singularities are prominent at the left and right extremes of the plot. The direct and exchange terms are plotted separately in figures 5 and 6. The total cross section at $2s_{\text{threshold}}$ is $\sigma(2s_t) = 40.2605$ mb. The total cross section σ is plotted in figure 7 as a function of s , and has a maximum of ~ 90 mb. Since the range of integration lies between the t and

u singularities, the *Mathematica* function *NIntegrate* is able to integrate the curve as a single piece, unlike the case involving $d\sigma/d\Omega_{3lab}$ (see section 3.6), where the singularity at θ_{peak} requires piecewise integration. σ goes to zero at $s_{\text{threshold}}$. As s increases, σ rises to a peak and then slowly diminishes with increasing s . These characteristics of the shape of the curve predicted by the scalar ABC theory agree with experiment as seen in reference [21] (figure 40.11).

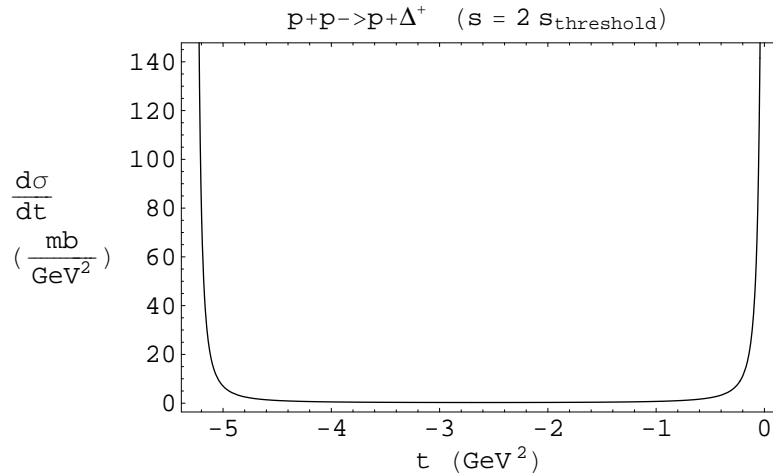


Figure 4: Differential cross section $d\sigma/dt$.

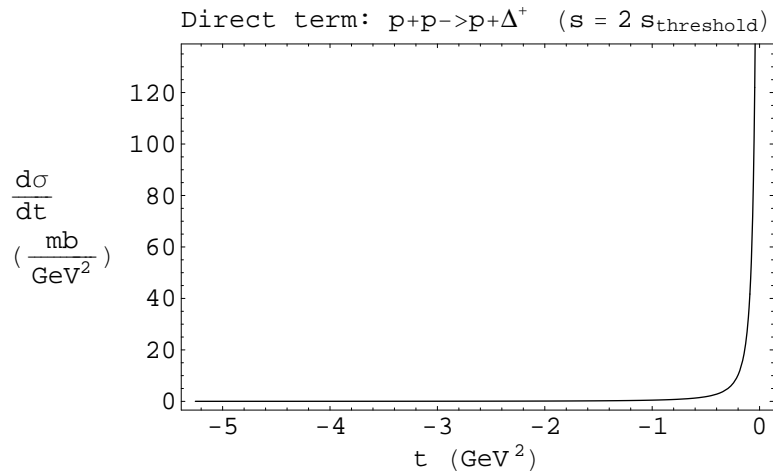


Figure 5: Differential cross section $d\sigma/dt$ direct term.

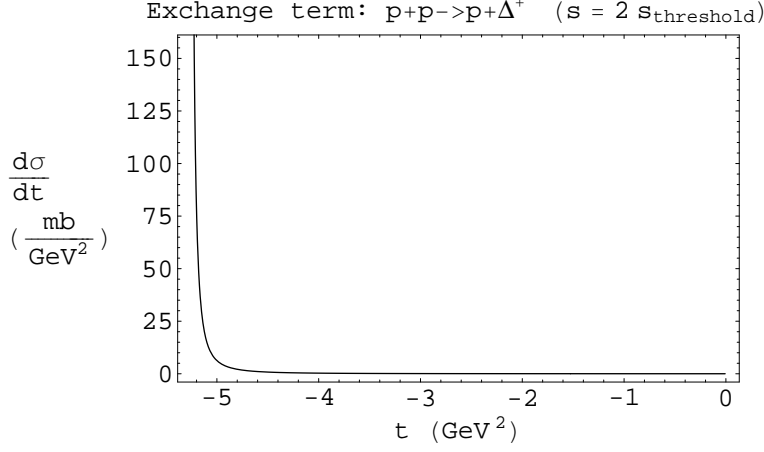


Figure 6: Differential cross section $d\sigma/dt$ exchange term.

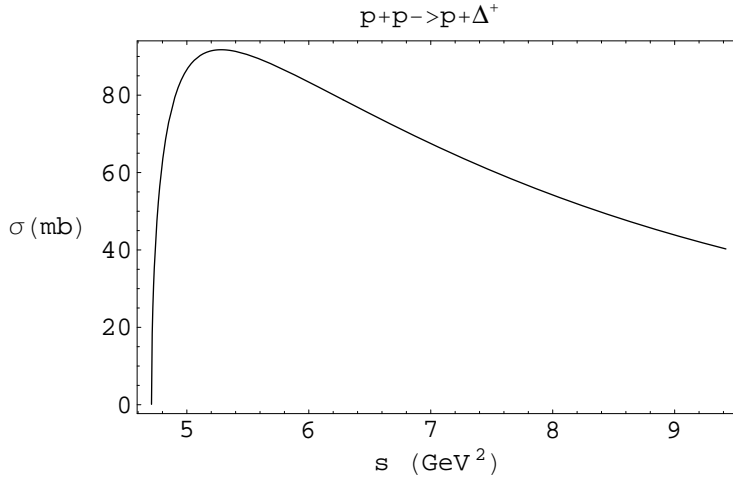


Figure 7: $pp \rightarrow p\Delta^+$ total cross section.

3.4 Angular distribution $d\sigma/d\Omega_c$ and σ in cm frame

The angular distribution in the cm frame will be developed in this subsection. For the 2 - body reaction $1 + 2 \rightarrow 3 + 4$, the angular distribution in the cm frame is given by equation (44),

$$\begin{aligned}
 \frac{d\sigma}{d\Omega_{cm}} &= \frac{\mathcal{S}}{64\pi^2 s} \sqrt{\frac{\lambda_{34}}{\lambda_{12}}} |\mathcal{M}|^2 \\
 &= \frac{1}{4\pi s} \sqrt{\lambda_{12}\lambda_{34}} \frac{d\sigma}{dt}, \tag{149}
 \end{aligned}$$

with

$$t = m_2^2 + m_4^2 + \frac{1}{2s} \left[-\sqrt{(\lambda_{12} + 4sm_2^2)(\lambda_{34} + 4sm_4^2)} + \sqrt{\lambda_{12}\lambda_{34}} \cos \theta_{24c} \right]. \quad (150)$$

See equation (45). In the cm frame, the angular distributions of particles 3 and 4 are equal [10],

$$d\sigma/d\Omega_{3c} \equiv d\sigma/d\Omega_{4c}. \quad (151)$$

Since both forms of the angular distribution above are functions of t , either may be used in conjunction with the expression $t(\theta_{24c})$ to give $d\sigma/d\Omega_{4c}$ as a function of θ_{24c} . The exchange particle is the π^0 . By setting the mass $m_4 = m_\Delta$, the mass of the Δ particle, we generate results for the reaction $pp \rightarrow p\Delta^+$. For the reaction $pp \rightarrow pp$, results are obtained by setting $m_4 = m_p$, the mass of the proton. In figure 8, the plot of $d\sigma/d\Omega_{4c}$ at $s = 2s_{\text{threshold}}$ exhibits a similar shape and the same symmetry as the plot of $d\sigma/dt$, noteworthy since one is a function of θ while the other is a function of t . Evaluating $d\sigma/d\Omega_{4c}$ at $\theta = 0$ and $\theta = \pi$ gives

$$\frac{d\sigma}{d\Omega_{4c}}(s = 2s_t, \theta = 0) = 318.376 \frac{\text{mb}}{\text{sr}}, \quad (152)$$

$$\frac{d\sigma}{d\Omega_{4c}}(s = 2s_t, \theta = \pi) = 318.376 \frac{\text{mb}}{\text{sr}}. \quad (153)$$

The total cross section σ is found by numerically integrating $d\sigma/d\Omega_{4c}$ over all possible final state angles $\theta = [0, \pi]$. At $s = 2s_t$, $\sigma(s = 2s_t) = 40.2605$ mb, which matches the previous result found by integrating $d\sigma/dt$. Figure 9 shows the total cross section $\sigma(s)$ over the range $s = [s_{\text{threshold}}, 2s_{\text{threshold}}]$. The plot is identical to the plot resulting from the integration of $d\sigma/dt$, as expected since total cross section is invariant.

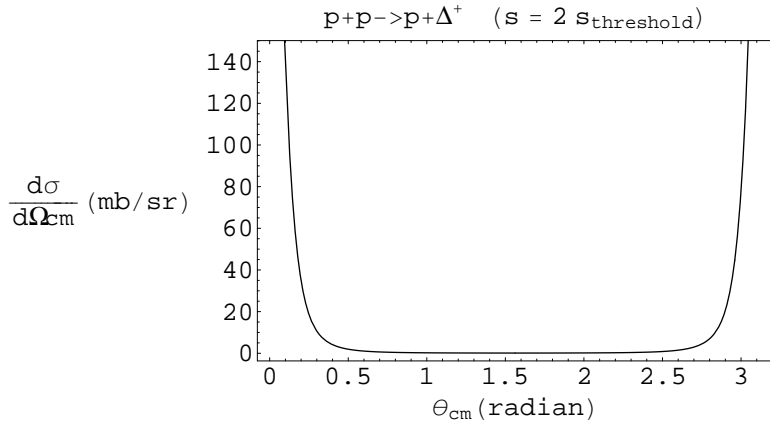


Figure 8: Differential cross section $d\sigma/d\Omega_{4c}$.

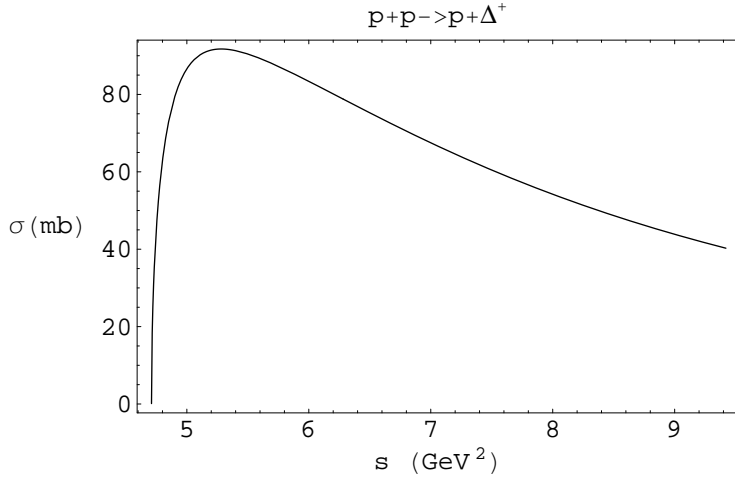


Figure 9: Total cross section σ .

3.5 Spectral distribution $d\sigma/dE_{3l}$ in the lab frame

In this subsection, the spectral distribution $d\sigma/dE_{3l}$ is derived from the invariant distribution $d\sigma/dt$ by expressing the invariants t and u in terms of the energy E and kinetic energy T , respectively (see Section 2.3.3). The formula is [10]

$$\frac{d\sigma}{dT_{3l}} = \frac{d\sigma}{dE_{3l}} = +2m_2 \frac{d\sigma}{dt}, \quad (154)$$

with t given by equation (37). The exchange particle is the π^0 . By setting the mass $m_4 = m_\Delta$, the mass of the Δ particle, we generate results for the reaction $pp \rightarrow p\Delta^+$. The results for the reaction $pp \rightarrow pp$ may be obtained by setting $m_4 = m_p$, the mass of the proton. The differential cross section $d\sigma/dE_{4l}$ is plotted at $s = 2s_{\text{threshold}}$. See figure 10. Note that in reference [10], it was shown that $dE_{3l} = -dE_{4l}$ and $dT_{3l} = -dT_{4l}$. Therefore, plotting $d\sigma/dE_{4l}$ is equivalent to plotting $d\sigma/dE_{3l}$. The plot range is found by inverting the formulas for t and u as functions of energy and evaluating them at t_0 and t_π . The plots have the characteristic horseshoe shape of the invariant distribution (which is plotted as a function of t). The total cross section is determined by numerically integrating the spectral distribution, and is plotted as a function of s over the range $s_{\text{threshold}}$ to $2s_{\text{threshold}}$. At $s = 2s_{\text{threshold}}$, the total cross section

$$\sigma(2s_t) = 40.2605 \text{ mb} \quad (155)$$

is identical to the value determined using the invariant distribution. Note that the two-body lab frame spectral distribution in equation (154) does not possess any singularity. Also, recall that a two-body cm frame spectral distribution is impossible to form because the cm energy of the final state particles are fixed [10]. In figures 4 and 5 of reference [22], Murphy, Dermer and Ramaty present cm and lab frame spectral distributions for the reaction $p + \alpha \rightarrow \pi^0 + X$. These are very useful data for future comparisons to theoretical models. Both spectral distributions

are finite and well behaved over the entire range of pion energy. However, the results above do not apply to this data because the reaction $p + \alpha \rightarrow \pi^0 + X$ is at least a 3-body final state.

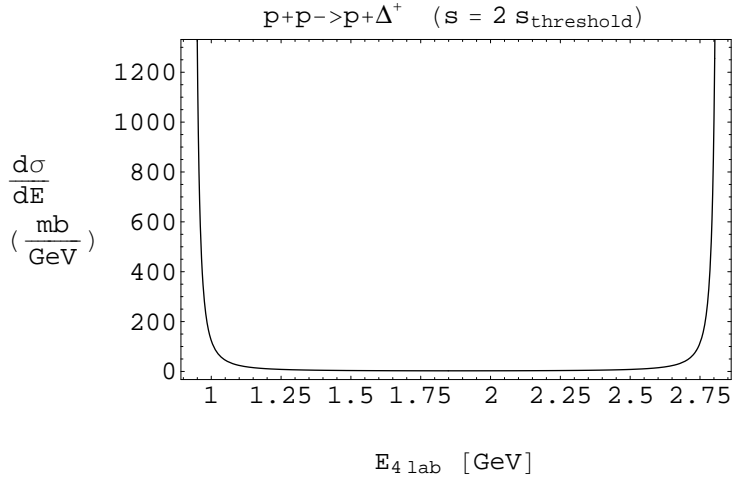


Figure 10: Differential cross section $d\sigma/dE_{4l}$.

3.6 Angular distribution $d\sigma/d\Omega_{3l}$ in lab frame

The angular distribution is required in the lab frame for space radiation studies. This is developed in the present subsection. The angular distribution $d\sigma/d\Omega_{3l}$ may be expressed in terms of the cm distribution $d\sigma/d\Omega_{3c}$. This is achieved by expressing t in terms of E_{3l} , and E_{3l} in terms of θ_{3l} . The exchange particle is the π^0 . By setting the mass $m_4 = m_\Delta$, the mass of the Δ particle, we generate results for the reaction $pp \rightarrow p\Delta^+$. The results for the reaction $pp \rightarrow pp$ may be obtained by setting $m_4 = m_p$, the mass of the proton. For the reaction $pp \rightarrow p\Delta^+$ with particle 3 the Δ^+ particle, the energy $E_{3l}(\theta_{3l})$ is a double valued function, except at θ_{peak} where the two energy roots are equal. In figure 11, the two E_{3l} roots are plotted piecewise together and join smoothly at $\theta_{3l\text{peak}}$ forming a single curve. $E_{3l\text{root1}}(\theta)$ forms the upper part of the curve, while $E_{3l\text{root2}}(\theta)$ forms the lower part of the curve. Since $E_{3l\text{root1}}(\theta_{\text{peak}}) = E_{3l\text{root2}}(\theta_{\text{peak}})$, θ_{peak} is found by setting the square root term in the numerator of (51) equal to zero and solving for θ . The slope of E_{3l} goes to infinity at θ_{peak} . This causes a singularity in $d\sigma/d\Omega_{3l}$ at θ_{peak} . The presence of the singularity is demonstrated by expressing $d\sigma/d\Omega_{3l}$ in terms of $dE/d\theta$,

$$\frac{d\sigma}{d\Omega_{3l}} = \frac{d\sigma}{d(\cos\theta)d\phi} = \frac{d\sigma}{dE} \frac{1}{(-\sin\theta)} \frac{dE}{d\theta}. \quad (156)$$

$d\sigma/dE_{3l}$ is continuous over the allowed range of E_{3l} (and corresponding range of θ), and $1/\sin\theta_{\text{peak}}$ is finite at θ_{peak} , whereas $dE/d\theta \rightarrow \infty$ at θ_{peak} . Physically, a narrow detector situated at an angle $\theta < \theta_{\text{peak}}$ will detect particles at two energies. The double valued nature of $E_{3l}(\theta)$ necessitates that $d\sigma/d\Omega_{3l}$ be evaluated in two parts, one part as a function of $E_{3l\text{root1}}$, the other of $E_{3l\text{root2}}$. $d\sigma/d\Omega_{3l}$ is the sum of the two parts. This process represents the adding

together of the contributions to the differential cross section of distinct states, which are physically distinguished by their different energies. The cross sections are added together only after their respective amplitudes are squared. In figure 12, the plot of $d\sigma/d\Omega_{3l}$ shows the singularity at $\theta_{3l\text{peak}} \simeq .744$. The partial cross section $\Delta\sigma$ is defined to be the cross section integrated over a finite small angular range. In figure 13, the detector plot shows the partial cross section $\Delta\sigma$ seen by a narrow detector of angular width $\Delta\theta = .01745$, positioned at angles θ_{3l} ranging from 0 to $\theta_{3l\text{peak}}$. The plot reveals an increase in the partial cross section near $\theta_{3l\text{peak}}$. The relativistic kinematics predict a bump in the lab angular distribution in the vicinity of $\theta_{3l\text{peak}}$. The plots of t and u as functions of θ_{3l} support the discussion about direct and exchange terms in section 2.3.1. For a given angle θ_{3l} and energy E_{3l} , there corresponds two unique values of t , and of u .

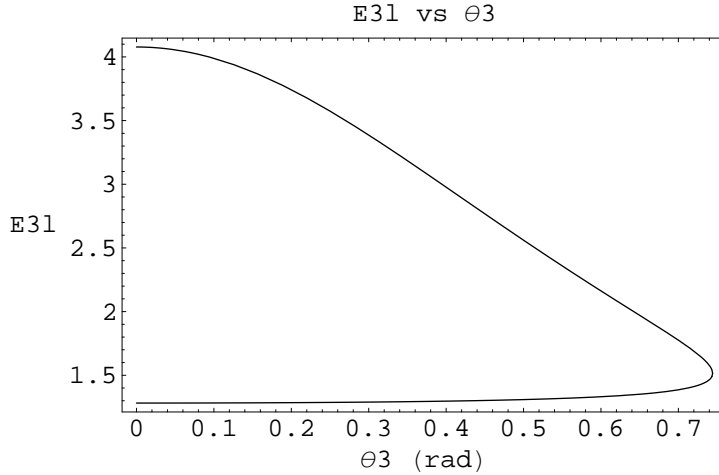


Figure 11: Energy $E_{3l}(\theta_{3l})$. Upper and lower parts of the curve correspond to E_{3l} roots 1 and 2, respectively.

3.6.1 Relation between cm and lab angles

In the cm frame, particles 3 and 4 exit from the collision in opposite directions, at angles ranging from 0 to 2π . Angles are measured with respect to the collision axis (particle 1 moves parallel to the collision axis in both frames, particle 2 is at rest in the lab frame but moves parallel to the collision axis in the cm frame). Due to symmetry about the collision axis, only angles between 0 and π need be considered. When viewed from the lab frame, the exit angles of particle 3 and 4 differ from the cm angles as shown in figure 14, where cm angles are transformed into corresponding lab angles. The difference in angles between the cm and lab frames is due to the relative velocity of the two frames, which affects the component of particle momentum along the collision axis, but not the component transverse to the axis. Also, see figures 15 and 16 which show the Mandelstam variables as a function of lab angle.

For the reaction $p + p \rightarrow p + \Delta^+$, with particles labeled $1 + 2 \rightarrow 3 + 4$, the velocities of initial state particles 1 and 2 in the cm frame are equal and opposite, and the velocity of particle

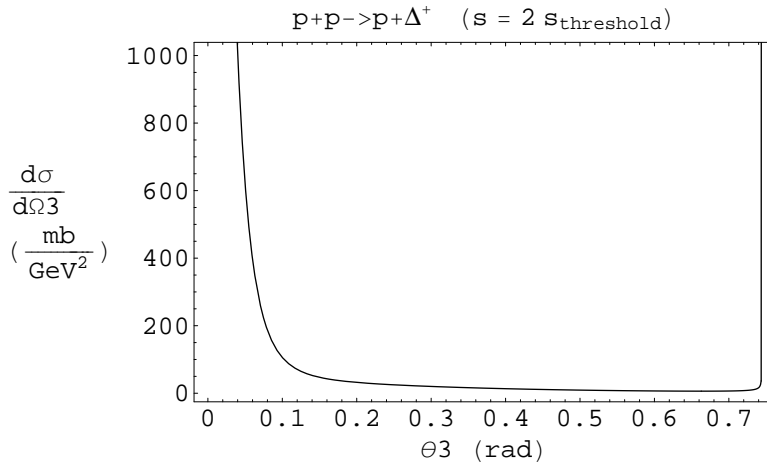


Figure 12: Differential cross section $d\sigma/d\Omega_{3l}$.

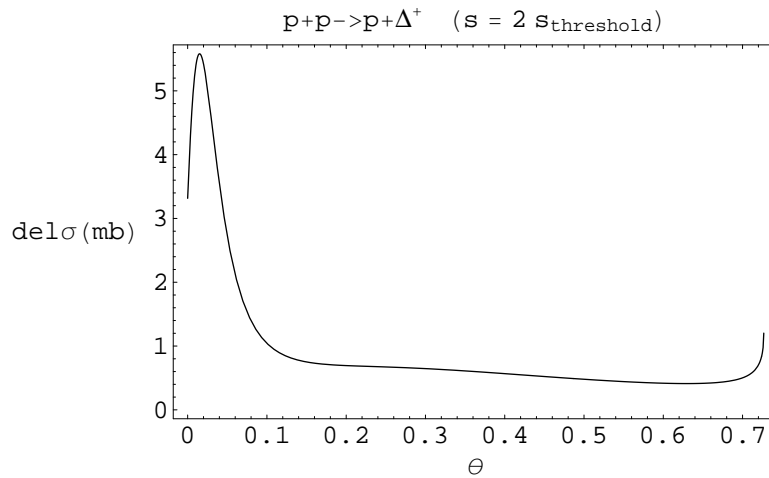


Figure 13: Detector partial cross section.

2 is equal to the velocity in the lab frame. In the cm frame, the momenta of the final state particles 3 and 4 are equal and opposite, but the velocities differ, thus the speed of the lab frame may be less than or greater than the speed of a final state particle. For the case of particles 3 and 4 exiting along the collision axis (with angles of 0 and π), this means that in transforming angles from cm to lab frame, the direction of a particle may be reversed (the particle with angle $\theta_{cm} = 0$ in the cm frame may have angle $\theta_{lab} = \pi$ in the lab frame). For all other angles, the transform from the cm frame to the lab frame reduces the angles, that is $\theta_{lab} < \theta_{cm}$. The effect of transforming the angles on the angular distributions is seen by comparing figure 8 with 12.

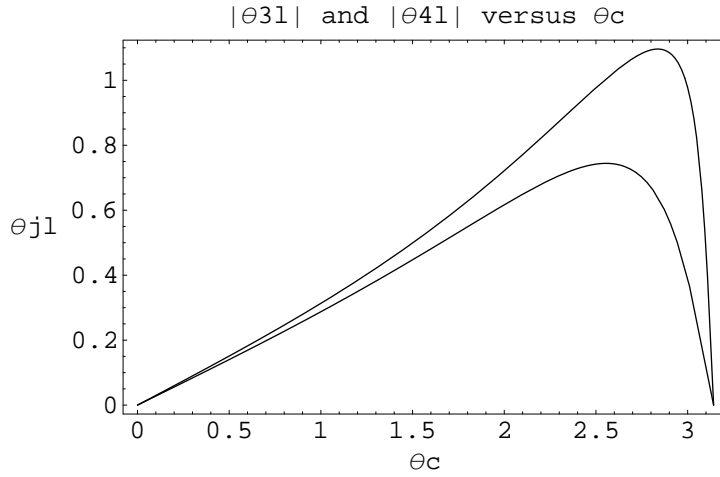


Figure 14: Angles θ_{3lab} and θ_{4lab} versus θ_{cm} .

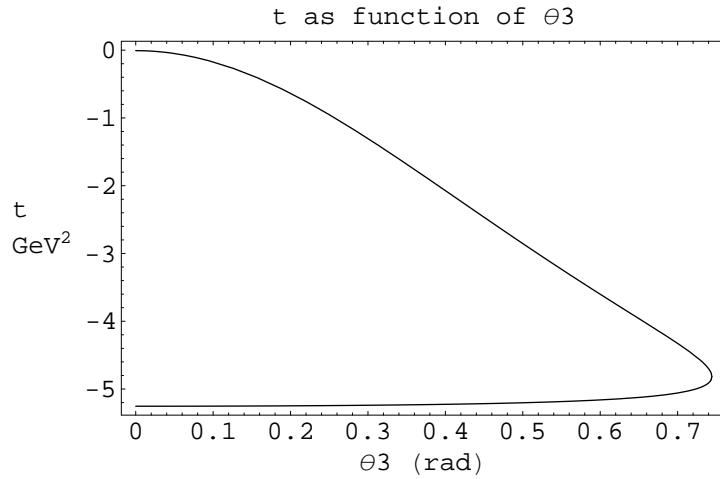


Figure 15: Mandelstam variable t as a function of θ_{3l} .

3.7 Calculations for zero-mass exchange particle (Rutherford scattering)

Previous sections were concerned with massive particle exchange. In this subsection, it is shown how to handle massless particle exchange. In Rutherford scattering, for the case of initial and final state particles having the same mass, the exchange particle has a mass $m = 0$, and the coupling is electromagnetic with coupling constant $g_{\gamma NN} = \alpha$ (in place of the pion coupling constant $g_{\pi NN}$). The exchange particle is the photon γ with mass $m = 0$. For $pp \rightarrow p\Delta$

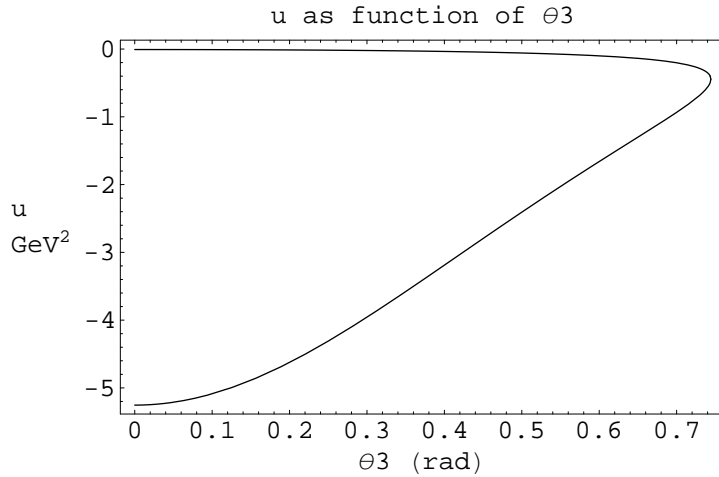


Figure 16: Mandelstam variable u as a function of θ_{3l} .

(non-Rutherford), evaluating $d\sigma/dt$ at t_0 and t_π at $s = 2s_{\text{threshold}}$ gives

$$\frac{d\sigma}{dt}(s = 2s_{\text{threshold}}, t = t_0) = 7.59 \frac{\text{pb}}{\text{GeV}^2}, \quad (157)$$

$$\frac{d\sigma}{dt}(s = 2s_{\text{threshold}}, t = t_\pi) = 7.59 \frac{\text{pb}}{\text{GeV}^2}. \quad (158)$$

For $pp \rightarrow pp$ (Rutherford), these cross sections are infinite due to the t and u singularities at $t = t_0$ and $t = t_\pi$. The physical explanation of this is that scattering always takes place when there is a potential of infinite range. Figures 17 and 18 plot the differential cross sections $d\sigma/dt$ and $d\sigma/d\Omega_{cm}$ for $pp \rightarrow p\Delta^+$. Figures 19 and 20 plot the differential cross sections for $pp \rightarrow pp$. Figure 21 plots the total cross section for $pp \rightarrow p\Delta^+$ (non-Rutherford). For $pp \rightarrow pp$ (Rutherford), the total cross section is infinite, in agreement with the classical result.

3.8 Comparison of cross sections

In this subsection, different forms of the cross section will be compared. The relative strengths of interaction processes $pp \rightarrow pp$ and $pp \rightarrow p\Delta^+$, both for massive and zero-mass exchange particles, are shown by comparing plots of the cross sections. For Rutherford scattering, the total cross section is infinite and cannot be plotted. Figure 22 compares plots of total cross sections for the elastic $pp \rightarrow pp$ and inelastic $pp \rightarrow p\Delta^+$ processes involving a massive (pion) exchange particle, over the energy range $s_{\text{threshold}}$ to $2s_{\text{threshold}}$. The elastic process dominates at low energies. Figures 23 and 24 plot the invariant cross sections of the elastic process $pp \rightarrow pp$ for massive (pion) and zero-mass (photon) exchange particle. Judging by the vertical axis scales, the strength of the pion process is many orders of magnitude greater than the photon process over the valid range of variable t . The plots are limited in height, and do not reveal the full story. The Rutherford invariant cross section goes to infinity at the limits t_0 and t_π , whereas the pion

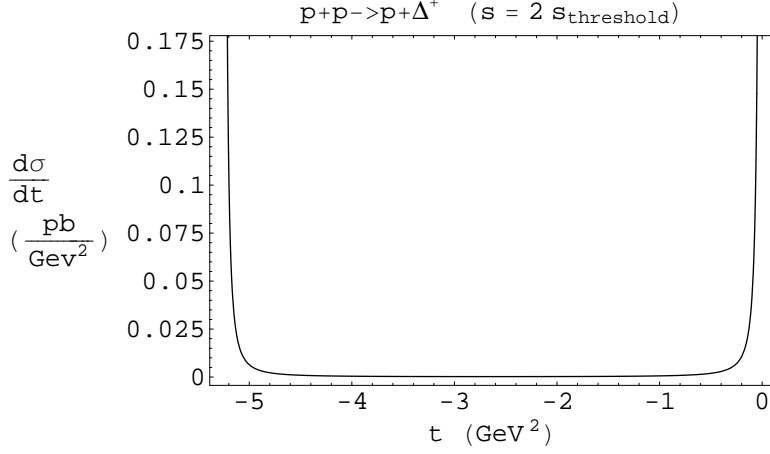


Figure 17: Invariant differential cross section (non-Rutherford).

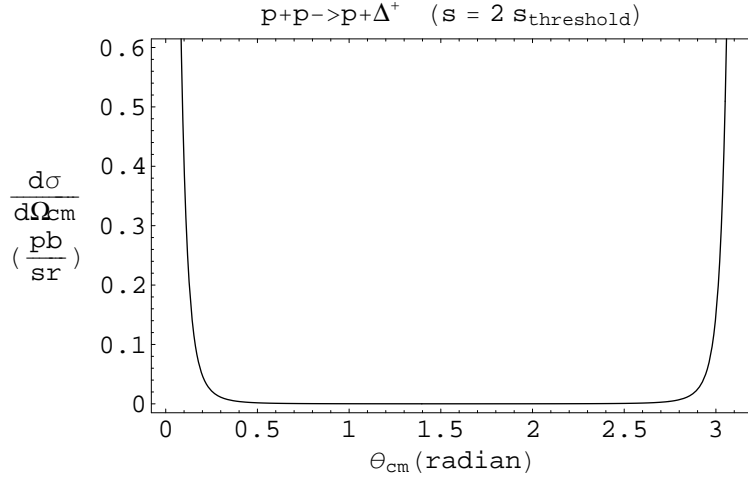


Figure 18: $d\sigma/d\Omega_{cm}$ Differential cross section (non-Rutherford).

invariant cross section is finite at the limits, $d\sigma/dt = 37.7 \text{ mb/GeV}^2$. Similar statements apply to the cm frame angular distributions, which are closely related to the t distributions since t varies linearly with $\cos \theta$. See equation (45). For most of the allowed range of angles 0 to π , the angular distribution of the pion process is many orders of magnitude greater than the photon process. However, at angles 0 and π , the Rutherford angular distribution goes to infinity. This is apparent by equation (81).

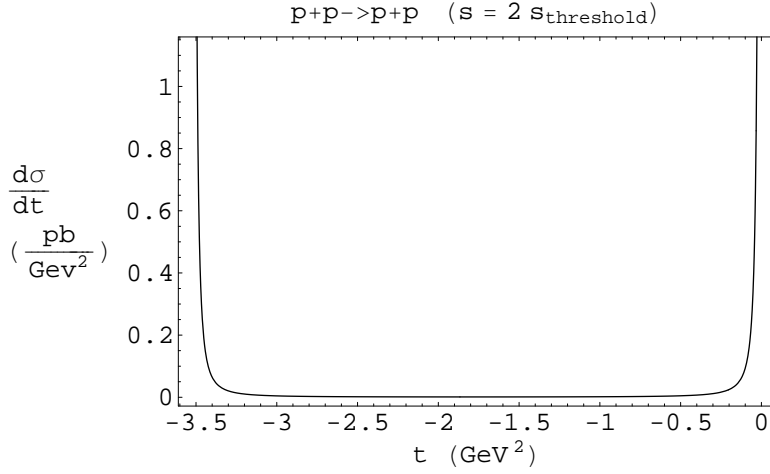


Figure 19: Invariant differential cross section (Rutherford).

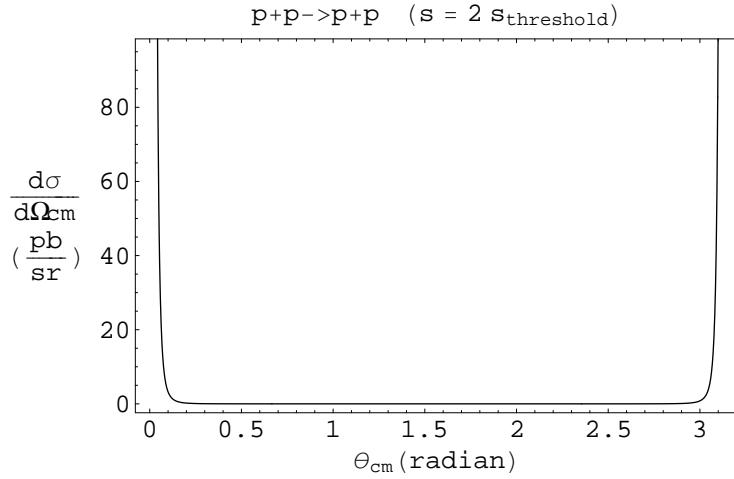


Figure 20: $d\sigma/d\Omega_{cm}$ Differential cross section (Rutherford)

4 Scattering for 3 - body final states

In this section, the formalism for describing 3 - body final state reactions will be presented. Cross sections will be calculated and special attention will be paid to the intermediate resonance formation and decay. Approximate techniques for handling resonance decay will be introduced. These results are important because many space radiation reactions include three or more bodies in the final state. The reaction

$$NN \rightarrow NN\pi, \quad (159)$$

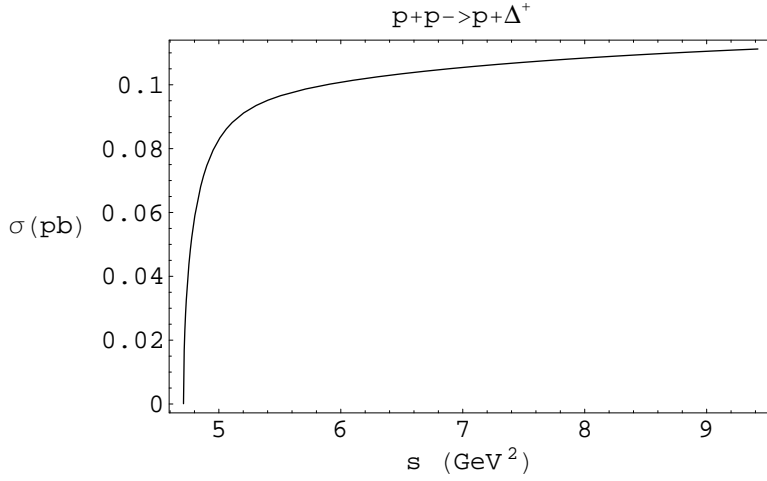


Figure 21: Total cross section (non-Rutherford).

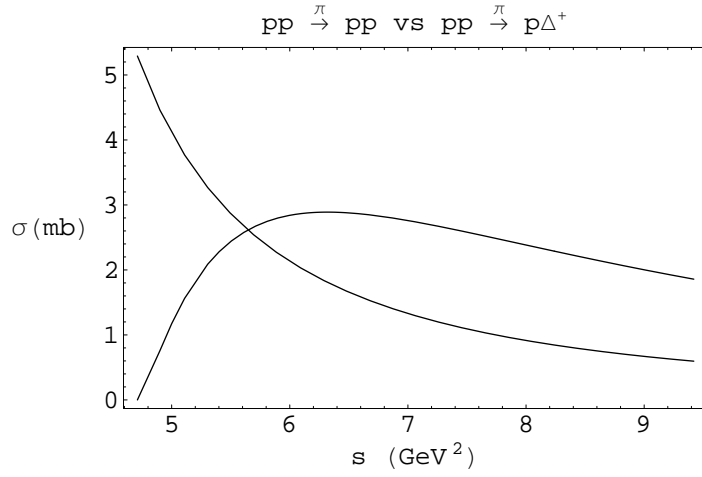


Figure 22: Comparison of elastic and inelastic total cross sections. The steadily falling cross section is elastic, and the cross section which rises and then falls is inelastic.

proceeds through Δ resonance formation

$$NN \rightarrow N\Delta \rightarrow NN\pi . \quad (160)$$

The Feynman diagram for this reaction is shown in figure 25. Thus, the reaction proceeds in two steps, namely

$$NN \rightarrow N\Delta , \quad (161)$$

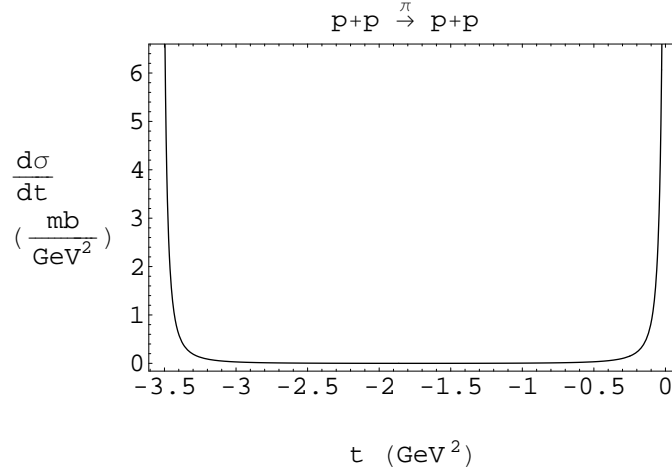


Figure 23: Invariant distribution for $pp \rightarrow pp$ by pion exchange.

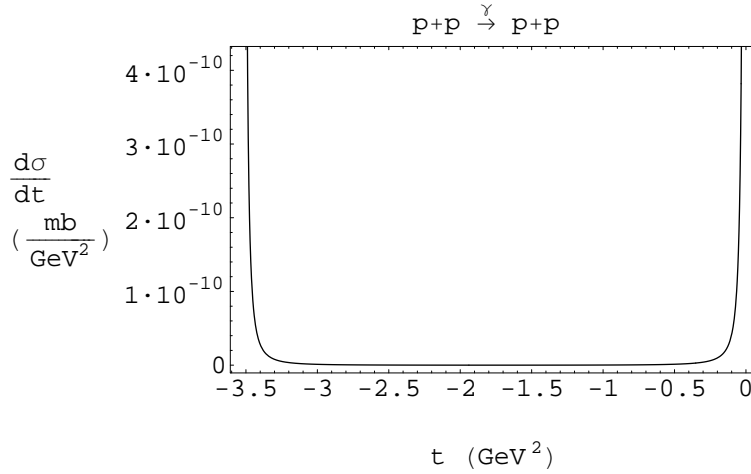


Figure 24: Invariant distribution for $pp \rightarrow pp$ by photon exchange.

and

$$\Delta \rightarrow N\pi . \tag{162}$$

4.1 Amplitude for Δ resonance formation and decay

An essential piece to the calculation of 3 - body final state cross sections, is the amplitude for resonance formation and decay. This is considered in the present subsection. The amplitude for the reaction in equation (159) is written in terms of the amplitudes in equations (161) and (162).

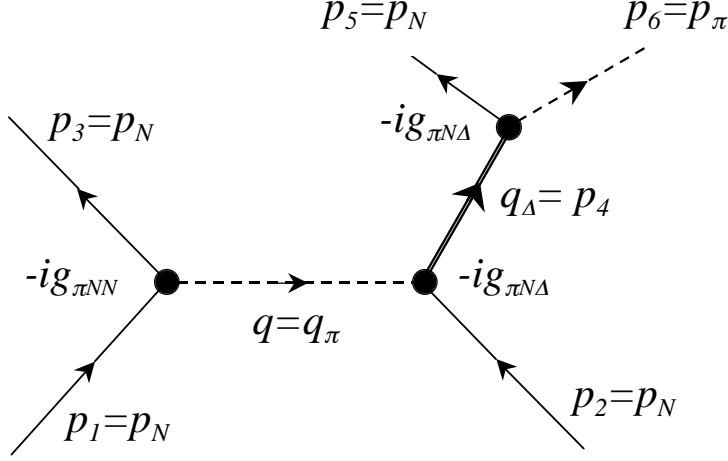


Figure 25: The Feynman diagram for the reaction $NN \rightarrow N\Delta \rightarrow NN\pi$. Note the labeling of the particle numbers. The initial state nucleons are labeled as particles 1 and 2. The final state nucleons are labeled as particles 3 and 5. The intermediate Δ state is labeled as particle 4, and the final produced π is labeled as particle 6.

Consider the complete reaction $NN \rightarrow N\Delta \rightarrow NN\pi$. The Feynman diagram is illustrated in figure 25. Using the Feynman rules for ABC (scalar) theory gives the amplitude

$$\begin{aligned}
& i\mathcal{M}(2\pi)^4\delta^4(p_1 + p_2 - p_3 - p_5 - p_6) \\
&= (-ig_{\pi NN})(-ig_{\pi N\Delta})^2(2\pi)^4\delta^4(p_1 - p_3 - q_\pi)(2\pi)^4\delta^4(q_\pi + p_2 - q_\Delta)(2\pi)^4\delta^4(q_\Delta - p_5 - p_6) \\
&\quad \times \frac{1}{(2\pi)^4} \int d^4q_\pi \frac{1}{(2\pi)^4} \int d^4q_\Delta \frac{i}{q_\pi^2 - m_\pi^2} \frac{i}{q_\Delta^2 - m_\Delta^2} \\
&= (-ig_{\pi NN})(-ig_{\pi N\Delta})^2(2\pi)^4\delta^4(p_1 - p_3 + p_2 - q_\Delta)(2\pi)^4\delta^4(q_\Delta - p_5 - p_6) \\
&\quad \times \frac{1}{(2\pi)^4} \int d^4q_\Delta \frac{i}{(p_1 - p_3)^2 - m_\pi^2} \frac{i}{q_\Delta^2 - m_\Delta^2} \\
&= (-ig_{\pi NN})(-ig_{\pi N\Delta})^2(2\pi)^4\delta^4(p_1 - p_3 + p_2 - p_5 - p_6) \\
&\quad \times \frac{i}{(p_1 - p_3)^2 - m_\pi^2} \frac{i}{(p_5 - p_6)^2 - m_\Delta^2}, \tag{163}
\end{aligned}$$

which reduces to

$$\begin{aligned}
& i\mathcal{M}(1 + 2 \rightarrow 3 + 5 + 6) = i\mathcal{M}(NN \rightarrow NN\pi) \\
&= (-ig_{\pi NN})(-ig_{\pi N\Delta})^2 \frac{i}{q_\pi^2 - m_\pi^2} \frac{i}{q_\Delta^2 - m_\Delta^2}, \quad (\text{with } q_\pi \equiv p_1 - p_3 \text{ and } q_\Delta \equiv p_5 - p_6). \tag{164}
\end{aligned}$$

Now consider the simpler reaction $NN \rightarrow N\Delta$. The Feynman diagram is illustrated in figure 26. The amplitude is

$$\begin{aligned}
& i\mathcal{M}(2\pi)^4\delta^4(p_1 + p_2 - p_3 - p_4) \\
&= (-ig_{\pi NN})(-ig_{\pi N\Delta})(2\pi)^4\delta^4(p_1 - p_3 - q_\pi)(2\pi)^4\delta^4(q_\pi + p_2 - p_4) \\
&\quad \times \frac{1}{(2\pi)^4} \int d^4q_\pi \frac{i}{q_\pi^2 - m_\pi^2} \\
&= (-ig_{\pi NN})(-ig_{\pi N\Delta})(2\pi)^4\delta^4(p_1 - p_3 + p_2 - p_4) \frac{i}{(p_1 - p_3)^2 - m_\pi^2}, \tag{165}
\end{aligned}$$

which reduces to

$$\begin{aligned}
i\mathcal{M}(1 + 2 \rightarrow 3 + 4) &= i\mathcal{M}(NN \rightarrow N\Delta)dLips \\
&= (-ig_{\pi NN})(-ig_{\pi N\Delta}) \frac{i}{q_\pi^2 - m_\pi^2}, \quad (\text{with } q_\pi \equiv p_1 - p_3). \tag{166}
\end{aligned}$$

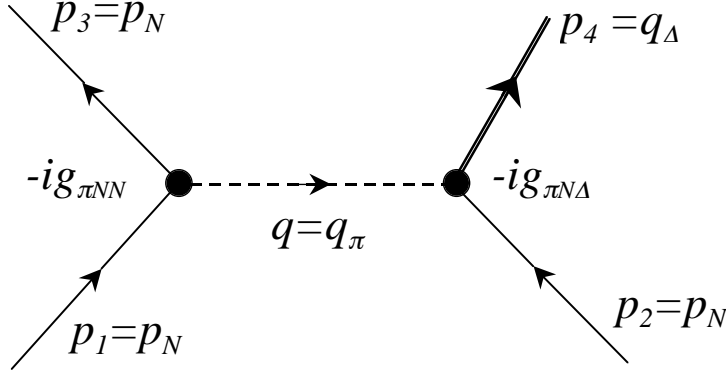


Figure 26: The Feynman diagram for the reaction $NN \rightarrow N\Delta$.

Now consider the decay $\Delta \rightarrow N\pi$. The Feynman diagram is illustrated in figure 27. The amplitude is

$$i\mathcal{M}(2\pi)^4\delta^4(p_4 - p_5 - p_6) = (-ig_{\pi N\Delta})(2\pi)^4\delta^4(p_4 - p_5 - p_6), \tag{167}$$

which reduces to

$$i\mathcal{M}(\Delta \rightarrow N\pi) = -ig_{\pi N\Delta}. \tag{168}$$

Combining the above equations (164), (166) and (168) gives

$$i\mathcal{M}(NN \rightarrow NN\pi) = i\mathcal{M}(\Delta \rightarrow N\pi) \frac{i}{q_\Delta^2 - m_\Delta^2} i\mathcal{M}(NN \rightarrow N\Delta). \tag{169}$$

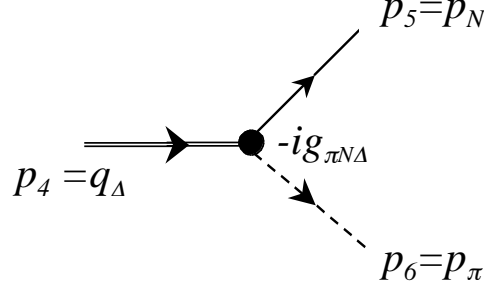


Figure 27: The Feynman diagram for the decay $\Delta \rightarrow N\pi$.

Thus,

$$|\mathcal{M}_{12 \rightarrow 356}|^2 = |\mathcal{M}_{4 \rightarrow 56}|^2 \frac{1}{(p_4^2 - m_4^2)^2} |\mathcal{M}_{12 \rightarrow 34}|^2 . \quad (170)$$

The equations (169) and (170) express the amplitude of the complete process in terms of the sub-processes.

4.2 Cross section for resonance formation and decay

The amplitude of the preceding section is now used to determine the cross section. In the following discussion, all statistical factors are $\mathcal{S} = 1$. Note that for $NN \rightarrow NN\pi$, $\mathcal{S} = 1/2$. From reference [10], the cross sections are

$$d\sigma(1 + 2 \rightarrow 3 + 5 + 6) = \frac{1}{4F} |\mathcal{M}_{12 \rightarrow 356}|^2 (2\pi)^4 d\Phi_3(p_1 + p_2; p_3, p_5, p_6) , \quad (171)$$

and

$$d\sigma(1 + 2 \rightarrow 3 + 4) = \frac{1}{4F} |\mathcal{M}_{12 \rightarrow 34}|^2 (2\pi)^4 d\Phi_2(p_1 + p_2; p_3, p_4) . \quad (172)$$

The phase space factor $d\Phi_n$ is given in reference [10]. From reference [10], the decay width is

$$d\Gamma(4 \rightarrow 5 + 6) = \frac{1}{2m_4} |\mathcal{M}_{4 \rightarrow 56}|^2 (2\pi)^4 d\Phi_2(p_4; p_5, p_6) . \quad (173)$$

From reference [10], the phase space recurrence relation is

$$d\Phi_3(P; p_1, p_2, p_3) = d\Phi_2(P; q, p_3) d\Phi_2(q; p_1, p_2) (2\pi)^3 dq^2 , \quad (174)$$

giving the phase space factor in equation (171) as (see proof in Section 4.4),

$$d\Phi_3(p_1 + p_2; p_3, p_5, p_6) = d\Phi_2(p_1 + p_2; p_4, p_3) d\Phi_2(p_4; p_5, p_6) (2\pi)^3 dp_4^2 . \quad (175)$$

Substituting equations (170) and (175) into equation (171) gives

$$\begin{aligned}
d\sigma(12 \rightarrow 356) &= \frac{1}{4F} |\mathcal{M}_{4 \rightarrow 56}|^2 \frac{1}{(p_4^2 - m_4^2)^2} |\mathcal{M}_{12 \rightarrow 34}|^2 (2\pi)^4 \\
&\quad \times d\Phi_2(p_1 + p_2; p_4, p_3) d\Phi_2(p_4; p_5, p_6) (2\pi)^3 dp_4^2 \\
&= d\sigma(12 \rightarrow 34) \frac{2m_4}{(2\pi)^4} d\Gamma(4 \rightarrow 56) \frac{1}{(p_4^2 - m_4^2)^2} (2\pi)^3 dp_4^2, \tag{176}
\end{aligned}$$

or

$$d\sigma(12 \rightarrow 356) = d\sigma(12 \rightarrow 34) d\Gamma(4 \rightarrow 56) \frac{m_4}{\pi} \frac{1}{(p_4^2 - m_4^2)^2} dp_4^2. \tag{177}$$

Integration of $d\sigma$ and $d\Gamma$ gives

$$\sigma(12 \rightarrow 356) = \int dp_4^2 \sigma(12 \rightarrow 34) \frac{m_4 \Gamma(4 \rightarrow 56) / \pi}{(p_4^2 - m_4^2)^2}. \tag{178}$$

De Wit [23] (p. 111) and Pilkuhn [18] (p. 36) have taken into account the decay width of the intermediate Δ resonance by the substitution

$$\frac{1}{p^2 + m^2} \rightarrow \frac{1}{p^2 + m^2 - im\Gamma}. \tag{179}$$

Here, Γ is distinguished from the $\Gamma(4 \rightarrow 56)$ of equations (173) and (176) by

$$\Gamma(4 \rightarrow 56) = \text{partial width}, \tag{180}$$

$$\Gamma = \text{total width}, \tag{181}$$

where the total width includes all possible decay paths. However, the propagators used in the present work are defined with a different sign, and therefore the above substitution becomes

$$\frac{1}{p_4^2 - m_4^2} \rightarrow \frac{1}{p_4^2 - m_4^2 - im_4\Gamma}. \tag{182}$$

The square of a complex number is $(x + iy)^2 = x^2 + y^2$ so that

$$\frac{1}{(p_4^2 - m_4^2)^2} \rightarrow \frac{1}{(p_4^2 - m_4^2)^2 + m_4^2 \Gamma^2}, \tag{183}$$

The differential cross section in equation (177) becomes

$$d\sigma(12 \rightarrow 356) = d\sigma(12 \rightarrow 34) d\Gamma(4 \rightarrow 56) \frac{m_4}{\pi} \frac{1}{(p_4^2 - m_4^2)^2 - (m_\Delta \Gamma)^2} dp_4^2, \tag{184}$$

and the total cross section in equation (178) becomes

$$\sigma(12 \rightarrow 356) = \int dp_4^2 \sigma(12 \rightarrow 34) \frac{m_4 \Gamma(4 \rightarrow 56) / \pi}{(p_4^2 - m_4^2)^2 + m_4^2 \Gamma^2}. \tag{185}$$

This can be re-written using [24]

$$\rho(\mu^2) \equiv \frac{m_4 \Gamma / \pi}{(\mu^2 - m_4^2)^2 + m_4^2 \Gamma^2}, \quad (186)$$

where $\mu^2 \equiv p_4^2$, to give

$$\sigma(12 \rightarrow 356) = \int d\mu^2 \sigma(12 \rightarrow 34) \rho(\mu^2) \frac{\Gamma(4 \rightarrow 56)}{\Gamma}. \quad (187)$$

Relabeling $p_4^2 \equiv x$, the integral above is simply

$$\int dx \frac{1}{(x - m^2)^2 + m^2 \Gamma^2}. \quad (188)$$

See section 4.2.2 below for an alternate derivation of equations (184) and (185).

4.2.1 Integration bounds on p_4^2

In equation (185), the upper integration bound on the value of p_4^2 is imposed by \sqrt{s} , the total center of momentum energy of the interaction. In the reaction $12 \rightarrow 34$, the square of the total center of momentum energy is given by

$$\begin{aligned} s &= (p_1 + p_2)^2 = (p_3 + p_4)^2 \\ &= m_3^2 + m_4^2 + 2E_3 E_4 - 2\mathbf{p}_3 \cdot \mathbf{p}_4 \\ &= m_3^2 + m_4^2 + 2E_3 E_4 + 2|\mathbf{p}_f|^2, \end{aligned} \quad (189)$$

where $\mathbf{p}_3 = -\mathbf{p}_4$ and $|\mathbf{p}_f| = |\mathbf{p}_3| = |\mathbf{p}_4|$. Equation (189) shows that for a given s , m_4^2 varies with $|\mathbf{p}_f|$, and has a maximum value when $|\mathbf{p}_f| = 0$, that is when all the mass and energy of particles 1 and 2 go into the mass of particles 3 and 4, with no kinetic energy remaining. In this case, $E_3 = m_3$, $E_4 = m_4$, and equation(189) becomes

$$s = (m_3 + m_4)^2. \quad (190)$$

Solving for m_4 , and noting that $p_4^2 \equiv m_4^2$

$$m_{4,\max} = \sqrt{s} - m_3, \quad (191)$$

$$x_{\max} = p_4^2 = (\sqrt{s} - m_3)^2. \quad (192)$$

The lower integration bound on the value of p_4^2 is imposed by the masses of the decay products of particle 4. In the reaction $12 \rightarrow 34 \rightarrow 356$, particle 4 decays by $4 \rightarrow 56$ into two real particles. For particle 4 to decay into particles 5 and 6, the mass of particle 4 must be at least as great as the sum of the masses of particles 5 and 6. Thus,

$$m_{4,\min} = m_5 + m_6. \quad (193)$$

This result can also be demonstrated as follows. In the rest frame of particle 4, the square of the center of momentum energy is

$$\begin{aligned}
s &= m_4^2 = (p_5 + p_6)^2 \\
&= m_5^2 + m_6^2 + 2E_5E_6 - 2\mathbf{p}_5 \cdot \mathbf{p}_6 \\
&= m_5^2 + m_6^2 + 2E_5E_6 + 2|\mathbf{p}_5|^2,
\end{aligned} \tag{194}$$

where the last step follows from $\mathbf{p}_6 \equiv -\mathbf{p}_5$. The minimum value of m_4 occurs when $|\mathbf{p}_5| = |\mathbf{p}_6| = 0$, in which case $E_5 = m_5$ and $E_6 = m_6$ and equation (194) reduces to

$$m_4^2 = (m_5 + m_6)^2, \tag{195}$$

which is equivalent to equation (193).

4.2.2 Alternate derivation of the cross section

An alternate, and better, derivation is now given. Equations (184) and (185) may also be derived by starting with the Feynman diagram for the 3 - body final state (figure 26) and noting that particle 4 is represented by an internal line (see Feynman Rules). This is a virtual particle whose mass m_4 can vary. Since particle 4 decays, it also has a decay width Γ . The internal decaying particle is described by the Breit-Wigner propagator [8] (p. 101), [16] (p. 163),

$$\text{Propagator} = \frac{i}{p_4^2 - m_4^2 - im_4\Gamma}. \tag{196}$$

The amplitude \mathcal{M} for the reaction $1 + 2 \rightarrow 4 + 5 + 6$ is then determined by applying the Feynman rules to figure 26, yielding

$$|\mathcal{M}|^2 = (g_{\pi NN} g_{\pi N\Delta}^2)^2 \frac{1}{(p_4^2 - m_\Delta^2)^2 + (m_\Delta\Gamma)^2} \left(\frac{1}{t - m_\pi^2} + \frac{1}{u - m_\pi^2} \right)^2. \tag{197}$$

Substituting the amplitude from equation (197) leads to equation (184), which may be expanded to

$$\begin{aligned}
d\sigma_{12 \rightarrow 456} &= \left(\frac{\mathcal{S}_{34}}{16\pi\lambda_{12}} |\mathcal{M}_{12 \rightarrow 34}|^2 dt \right) \left(\frac{\mathcal{S}_{56} |\mathbf{p}_5|}{8m_4^2 (2\pi)^2} |\mathcal{M}_{4 \rightarrow 56}|^2 d\Omega_5 \right) \\
&\quad \times \frac{m_4}{\pi} \frac{dp_4^2}{(p_4^2 - m_\Delta^2)^2 - (m_\Delta\Gamma)^2},
\end{aligned} \tag{198}$$

where

$$\begin{aligned}
m_\Delta &= \Delta \text{ resonance mass,} \\
\Gamma &= \Delta \text{ resonance width,} \\
m_4^2 &= p_4^2 \neq m_\Delta^2 \text{ in general,} \\
|\mathbf{p}_5| &= \frac{1}{2m_4} \sqrt{m_4^4 + m_5^4 + m_6^4 - 2(m_5^2 m_6^2 + m_5^2 m_4^2 + m_6^2 m_4^2)}.
\end{aligned}$$

The result for $|\mathbf{p}_5|$ is taken from reference [10]. \mathcal{S}_{34} and \mathcal{S}_{56} are the statistical factors associated with the sets of final state particles (3,4) and (5,6), respectively. For the reaction $NN \rightarrow N\Delta \rightarrow NN\pi$, both factors are unity. The integrals over dt and $d\Omega_5$ are performed holding m_4^2 constant. Since Γ is invariant (like rest mass, Γ is a rest width), the integral over $d\Omega_5$ is most easily performed in the cm frame for particle 4 and yields a factor of 4π . While the integral over dt is independent of p_4^2 , the integration bounds t_0 and t_π are functions of $m_4^2 (= p_4^2)$, so that integration over dt must precede integration over p_4^2 .

4.2.3 Narrow width approximation

Consider the approximation of a narrow width. A narrow width ($\Gamma \rightarrow 0$) corresponds to a long lifetime ($\tau \rightarrow \infty$). The narrow width approximation allows equation (186) to be simplified. The narrow width approximation gives [18] (p. 37)

$$\begin{aligned} \delta(x - m^2) &= \lim_{m\Gamma \rightarrow 0} \rho(x) \\ &= \lim_{m\Gamma \rightarrow 0} \frac{m\Gamma/\pi}{(x - m^2)^2 + m^2\Gamma^2} , \end{aligned} \quad (199)$$

so that equation (186) becomes

$$\sigma(12 \rightarrow 356) = \int d\mu^2 \sigma(12 \rightarrow 34) \delta(\mu^2 - m_4^2) \frac{\Gamma(4 \rightarrow 56)}{\Gamma} , \quad (200)$$

to finally give the cross section in the narrow width approximation [18] (p. 37),

$$\sigma(12 \rightarrow 356) = \sigma(12 \rightarrow 34) \frac{\Gamma(4 \rightarrow 56)}{\Gamma} . \quad (201)$$

A further simplification is achieved if the partial width is nearly equal to the total width, i.e.

$$\Gamma \approx \Gamma(4 \rightarrow 56) . \quad (202)$$

Then

$$\sigma(12 \rightarrow 356) \approx \sigma(12 \rightarrow 34) , \quad (203)$$

or

$$\sigma(NN \rightarrow NN\pi) \approx \sigma(NN \rightarrow N\Delta) . \quad (204)$$

This expression states that if the Δ resonance decays primarily to a particular final state $N\pi$, then the total cross section for π production is nearly the same as the total cross section for Δ production. Since the calculation of the cross section of a 2 - body final state $N\Delta$ is simpler than that of a 3 - body final state $NN\pi$, equation (204) is a considerable simplification in calculating the total cross section for π production.

4.3 $dLips$ formalism

In this subsection it will be shown how to develop useful formulas to handle Lorentz invariant phase space. Note that the above is discussed by [18] (pp. 16, 18) who uses a formalism involving the Lorentz invariant phase space $dLips(p_1, \dots, p_n)$. The result of Pilkuhn is easily shown to be identical to the result obtained here. We have the definition [18] (p. 16)

$$dLips(p_1 \dots p_n) \equiv \prod_{i=1}^n \frac{d^3 p_i}{(2\pi)^3 2E_i}, \quad (205)$$

and

$$\begin{aligned} dLips(s; p_1 \dots p_n) &= (2\pi)^4 \delta^4(P - \sum_i^n p_i) dLips(p_1 \dots p_n) \\ &= (2\pi)^4 \delta^4(P - \sum_i^n p_i) \prod_{i=1}^n \frac{d^3 p_i}{(2\pi)^3 2E_i} \\ &= (2\pi)^4 d\Phi_n(P; p_1 \dots p_n). \end{aligned} \quad (206)$$

The Pilkuhn recurrence formula is (with $s_d \equiv q^2 = (p_1 + p_2)^2$)

$$\begin{aligned} dLips(s; p_1, p_2, p_3) &= \frac{1}{2\pi} dLips(s; p_d, p_3) dLips(s_d; p_1, p_2) ds_d \\ = (2\pi)^4 d\Phi_3(P; p_1, p_2, p_3) &= \frac{1}{2\pi} (2\pi)^4 d\Phi_2(P; p_d, p_3) (2\pi)^4 d\Phi_2(q; p_1, p_2) dq^2, \end{aligned} \quad (207)$$

or

$$d\Phi_3(P; p_1, p_2, p_3) = (2\pi)^3 d\Phi_2(P; p_d, p_3) d\Phi_2(q; p_1, p_2) dq^2, \quad (208)$$

in agreement with equation (175).

4.4 Proof of phase space formula

We now prove the phase space formula in equation (175),

$$d\Phi_3(p_1 + p_2; p_3, p_5, p_6) = d\Phi_2(p_1 + p_2; p_4, p_3) d\Phi_2(p_4; p_5, p_6) (2\pi)^3 dp_4^2. \quad (209)$$

The proof proceeds as follows [18] (p. 18). The various phase space factors are

$$\begin{aligned} d\Phi_3(p_1 + p_2; p_3, p_5, p_6) &= \delta^4(p_1 + p_2 - p_3 - p_5 - p_6) \frac{d^3 p_3}{(2\pi)^3 2E_3} \frac{d^3 p_5}{(2\pi)^3 2E_5} \frac{d^3 p_6}{(2\pi)^3 2E_6}, \\ d\Phi_2(p_1 + p_2; p_4, p_3) &= \delta^4(p_1 + p_2 - p_4 - p_3) \frac{d^3 p_4}{(2\pi)^3 2E_4} \frac{d^3 p_3}{(2\pi)^3 2E_3}, \\ d\Phi_2(p_4; p_5, p_6) &= \delta^4(p_4 - p_5 - p_6) \frac{d^3 p_5}{(2\pi)^3 2E_5} \frac{d^3 p_6}{(2\pi)^3 2E_6}. \end{aligned}$$

d^3p refers to the volume element of a 3-vector and d^4p refers to the volume element of a 4-vector. However, when we write p^2 or dp^2 , then the p refers to a 4-vector, not a 3-vector! This is why some authors [24] prefer to write $dp^2 \equiv d\mu^2$ where μ is the mass, given by $p^2 = \mu^2 = E^2 - |\mathbf{p}|^2$. Using the identity

$$1 = d^4p_4 \delta^4(p_4 - p_5 - p_6) , \quad (210)$$

yields

$$\begin{aligned} d\Phi_3(p_1 + p_2; p_3, p_5, p_6) &= \delta^4(p_1 + p_2 - p_3 - p_5 - p_6) \frac{d^3p_3}{(2\pi)^3 2E_3} \\ &\quad \times d^4p_4 \delta^4(p_4 - p_5 - p_6) \frac{d^3p_5}{(2\pi)^3 2E_5} \frac{d^3p_6}{(2\pi)^3 2E_6} \\ &= \delta^4(p_1 + p_2 - p_3 - p_5 - p_6) \frac{d^3p_3}{(2\pi)^3 2E_3} d^4p_4 d\Phi_2(p_4; p_5, p_6) . \end{aligned}$$

Now using the result $1 = \delta(x - a)dx$ or

$$1 = \delta(p_4^2 - s_d) dp_4^2 \quad (211)$$

with [24] (equation 14), [18] (p. 15),

$$\begin{aligned} s_d &= (p_5 + p_6)^2 \\ &= (E_5 + E_6)^2 - (\mathbf{p}_5 + \mathbf{p}_6)^2 , \end{aligned} \quad (212)$$

gives

$$\begin{aligned} d^4p_4 &= d^4p_4 \delta(p_4^2 - s_d) dp_4^2 \\ &= \frac{d^3p_4}{2E_4} dp_4^2 = (2\pi)^3 \frac{d^3p_4}{(2\pi)^3 2E_4} dp_4^2 , \end{aligned} \quad (213)$$

where we have used the result

$$\frac{d^3p}{2E} = \delta(p^2 - m^2) d^4p . \quad (214)$$

Thus, the above phase space factor becomes

$$\begin{aligned} d\Phi_3(p_1 + p_2; p_3, p_5, p_6) &= \delta^4(p_1 + p_2 - p_3 - p_4) \frac{d^3p_3}{(2\pi)^3 2E_3} \frac{d^3p_4}{(2\pi)^3 2E_4} \\ &\quad \times dp_4^2 d\Phi_2(p_4; p_5, p_6) \\ &= d\Phi_2(p_1 + p_2; p_4, p_3) d\Phi_2(p_4; p_5, p_6) (2\pi)^3 dp_4^2 , \end{aligned} \quad (215)$$

which is the desired result.

The equation (214) used in the preceding step is derived as follows. Differentiating $p^2 = E^2 - \mathbf{p}^2$ gives

$$d^4p = dE d^3\mathbf{p} . \quad (216)$$

Expanding $\delta(p^2 - m^2)d^4p$ gives

$$\delta(p^2 - m^2)d^4p = \delta(E^2 - \mathbf{p}^2 - m^2)dE d^3\mathbf{p}. \quad (217)$$

Applying the formula

$$\delta(f(E)) = \sum_i \frac{1}{f'(E)} \delta(E - E_i), \quad (218)$$

with $f(E) = (E + \sqrt{\mathbf{p}^2 + m^2})(E - \sqrt{\mathbf{p}^2 + m^2})$, and keeping only the positive E root, gives

$$\delta(p^2 - m^2)d^4p = \delta(E - \sqrt{\mathbf{p}^2 + m^2})dE \frac{d^3\mathbf{p}}{2E}. \quad (219)$$

Integrating over dE cancels the delta function, leaving

$$\frac{d^3p}{2E} = \delta(p^2 - m^2)d^4p. \quad (220)$$

5 Conclusions

We have presented some applications of a scalar quantum field theory method by considering massive particle exchange, and we have calculated differential and total cross sections for elastic and inelastic processes. The use of Mandelstam variables makes the mathematical expressions much simpler. The cross section formulas are all obtained in closed form and are compact and simple. The cross sections display typical behavior of elastic and inelastic processes. The theory only includes the lowest order terms. At larger energies, higher order terms are expected to contribute. However, these complications may sometimes be circumvented by appropriate adjustment of parameters, such as the coupling constants. The theory developed herein will be useful in calculating cross sections for production of all types of hadrons, if the effects of spin can be neglected. These cross sections can then be included in space radiation transport codes.

References

- [1] F. A. Cucinotta, J. W. Wilson and J. W. Norbury, *Parameterizations of pion energy spectrum in nucleon - nucleon collisions*, NASA Technical memorandum 208722 (1998).
- [2] S. R. Blattnig, S. Swaminathan, A. T. Kruger, M. Ngom and J. W. Norbury, Phys. Rev. D **62**, 094030 (2000).
- [3] J. W. Norbury, S. R. Blattnig and R. Norman, *Cross - Section Parameterizations for Pion and Nucleon Production from Negative Pion - Proton Collisions*. NASA Technical Paper 211766 (2002).
- [4] S. R. Blattnig, J. W. Norbury, R. B. Norman, J. W. Wilson, R. C. Singleterry, and R. K. Tripathi, MESTRN: A Deterministic meson - muon transport code for space radiation. NASA Technical Memorandum 21995 (2004).

- [5] S. R. Blattnig, S. Swaminathan, A. T. Kruger, M. Ngom, J. W. Norbury and R. Tripathi, *Parameterized cross sections for pion production in proton - proton collisions*. NASA Technical Paper 210640 (2000).
- [6] R. Machleidt, *Advances in Nuclear Physics* **19**, 189 (1989).
- [7] D. Griffiths, *Introduction to elementary particles*. (Wiley, New York, 1987).
- [8] M. E. Peskin and D. V. Schroeder, *An introduction to quantum field theory*, (Perseus books, Reading, Massachusetts, 1995).
- [9] R. P. Feynman, R. B. Leighton and M. Sands, *The Feynman lectures on physics*, Vol. 3 (Addison - Wesley, Reading, Massachusetts, 1965).
- [10] J. W. Norbury and F. Dick, *Differential cross section kinematics for 3 - dimensional transport codes*. NASA Technical Paper 215543 (2008).
- [11] H. Goldstein, *Classical Mechanics*, 2nd ed., (Addison - Wesley, Reading, Massachusetts, 1980).
- [12] J. B. Marion, *Classical dynamics of particles and systems*, 3rd ed., (Harcourt, Brace, Jovanovich College Publishers, New York, 1988).
- [13] D. Bohm, *Quantum mechanics*, (Springer - Verlag, New York, 2001).
- [14] M. R. Spiegel, *Mathematical handbook*, Schaum Outline Series, (McGraw - Hill, New York, 1995).
- [15] H. Frauenfelder and E. M. Henley, *Subatomic physics*. 2nd ed., (Prentice - Hall, 1991).
- [16] M. Maggiore, *A modern introduction to quantum field theory*. (Oxford University Press, New York, 2005).
- [17] R. Machleidt and G. Q. Li, *Constraints on the πNN Coupling Constant from the NN System*, arXiv:nucl-th/9311012, (1993).
- [18] H. Pilkuhn, *The interactions of hadrons*, (North - Holland, Amsterdam, 1967).
- [19] J. D. Bjorken and S. D. Drell, *Relativistic quantum mechanics*, (McGraw - Hill, New York, 1964).
- [20] F. Halzen and A. D. Martin, *Quarks and leptons*, (Wiley, New York, 1984).
- [21] S. Eidelman *et al.*, *Physics Letters B* **592**, 1 (2004).
- [22] R. J. Murphy, C. D. Dermer, and R. Ramaty, *Astrophys. J. Suppl.* **63**, 721 (1987).
- [23] B. de Wit and J. Smith, *Field theory in particle physics*. (North-Holland, Amsterdam, 1986).
- [24] V. Dmitriev, O. Sushkov, and C. Gaarde, *Nucl. Phys. A* **459**, 503 (1986).

REPORT DOCUMENTATION PAGE

*Form Approved
OMB No. 0704-0188*

The public reporting burden for this collection of information is estimated to average 1 hour per response, including the time for reviewing instructions, searching existing data sources, gathering and maintaining the data needed, and completing and reviewing the collection of information. Send comments regarding this burden estimate or any other aspect of this collection of information, including suggestions for reducing this burden, to Department of Defense, Washington Headquarters Services, Directorate for Information Operations and Reports (0704-0188), 1215 Jefferson Davis Highway, Suite 1204, Arlington, VA 22202-4302. Respondents should be aware that notwithstanding any other provision of law, no person shall be subject to any penalty for failing to comply with a collection of information if it does not display a currently valid OMB control number.
PLEASE DO NOT RETURN YOUR FORM TO THE ABOVE ADDRESS.

1. REPORT DATE (DD-MM-YYYY) 01-12-2008			2. REPORT TYPE Technical Publication		3. DATES COVERED (From - To)	
4. TITLE AND SUBTITLE Cross Sections From Scalar Field Theory					5a. CONTRACT NUMBER	
					5b. GRANT NUMBER	
					5c. PROGRAM ELEMENT NUMBER	
6. AUTHOR(S) Dick, Frank; Norbury, John W.; Norman, Ryan B.; Nasto, Rachel					5d. PROJECT NUMBER	
					5e. TASK NUMBER	
					5f. WORK UNIT NUMBER 651549.02.07.01	
7. PERFORMING ORGANIZATION NAME(S) AND ADDRESS(ES) NASA Langley Research Center Hampton, VA 23681-2199					8. PERFORMING ORGANIZATION REPORT NUMBER L-19558	
9. SPONSORING/MONITORING AGENCY NAME(S) AND ADDRESS(ES) National Aeronautics and Space Administration Washington, DC 20546-0001					10. SPONSOR/MONITOR'S ACRONYM(S) NASA	
					11. SPONSOR/MONITOR'S REPORT NUMBER(S) NASA/TP-2008-215555	
12. DISTRIBUTION/AVAILABILITY STATEMENT Unclassified - Unlimited Subject Category 93 Availability: NASA CASI (301) 621-0390						
13. SUPPLEMENTARY NOTES						
14. ABSTRACT A one pion exchange scalar model is used to calculate differential and total cross sections for pion production through nucleon-nucleon collisions. The collisions involve intermediate delta particle production and decay to nucleons and a pion. The model provides the basic theoretical framework for scalar field theory and can be applied to particle production processes where the effects of spin can be neglected.						
15. SUBJECT TERMS Cross section; Pion; Scalar						
16. SECURITY CLASSIFICATION OF:			17. LIMITATION OF ABSTRACT	18. NUMBER OF PAGES	19a. NAME OF RESPONSIBLE PERSON	
a. REPORT	b. ABSTRACT	c. THIS PAGE			STI Help Desk (email: help@sti.nasa.gov)	
U	U	U	UU	55	19b. TELEPHONE NUMBER (Include area code) (301) 621-0390	